

3D-Gene[®] is a microarray technology developed by Toray. This technology has been applied for gene expression profiling and miRNA analysis (Sato et al. 2009; Sudo et al. 2012). 3D-Gene[®] microarray has a micro-columnar structure and uses a bead-agitation technique to achieve high sensitivity and reproducibility. Toray has established a new 3D-Gene[®] assay for the detection of *KRAS* mutations in tumor tissues using the PCR-rSSO (PCR-reverse sequence-specific oligonucleotide) method. Both Luminex and 3D-Gene[®] assays are based on the PCR-rSSO method. However, fluorescent beads are detected by flow cytometry in the Luminex assay. On the other hand, the 3D-Gene[®] assay utilizes array technology for the detection of the fluorescent PCR product. In this study, we compared the clinical performance of the 3D-Gene[®] mutation assay with two other assays (Scorpion-ARMS and Luminex) using FFPE tissue specimens from colorectal cancer patients (Harlé et al. 2013; Fukushima et al. 2011).

Results

Sensitivity of 3D-Gene[®] *KRAS* mutation assay

The minimum number of mutant DNA copies that were reliably detected by the 3D-Gene[®] assay was 350–700 copies (2.5–5%) as determined by using serially diluted mutant DNA (G12S) against wild-type DNA of HeLa cells (15000 copies; 50 ng). The minimum threshold for the number of mutant DNA copies was 700–1400 (5–10%) using serially diluted mutant DNA (G13D) against wild-type DNA of HeLa cells.

Study population

One hundred fifty FFPE tissue samples from patients with colorectal cancer in Kinki University Hospital, Faculty of Medicine were examined. All of the samples were available for analysis. The clinical and pathological characteristics are summarized in Additional file 1: Table S1.

Mutation types of *KRAS*

KRAS mutations were detected in 53/150 (36.0%), 53/150 (35.3%) and 51/150 (34.0%) cases by 3D-Gene[®], Scorpion-ARMS and Luminex, respectively. (Additional file 1: Table S2). Mutations were mainly located in codon 12 of *KRAS* (40/53, 75.5%). G12V mutations were most frequently observed by all assays (14/53, 26.4%). G13D was detected in 13 cases, but no other mutation in codon 13 was detected.

Invalid test rate

Mutation analysis of exons 12–13 of the *KRAS* gene was successfully performed in all 150 specimens (100%) using the 3D-Gene[®] mutation assay. No invalid test results were detected in the two other assays. The invalid test rate for this study was 0%.

Method correlation agreement analysis

We compared the *KRAS* mutation status across the three assays: 3D-Gene[®], Scorpion-ARMS, and Luminex. The correlation rates between 3D-Gene[®] and Scorpion-ARMS or 3D-Gene[®] and Luminex were 98.7% (148/150). The 3D-Gene[®] assay detected mutant *KRAS* in two specimens, but were wild-type by the Scorpion-ARMS method. Two specimens had a discrepant status between 3D-Gene[®] and Luminex. The first specimen had a wild-type *KRAS* by 3D-Gene[®] but was mutant by Luminex. Second specimen had a mutant *KRAS* by 3D-Gene[®] but was wild-type by Luminex. The concordance of the data from the three *KRAS* mutation assays is shown in Additional file 1: Tables S3 and S4. Only three discordant results between the three *KRAS* mutation assays were observed. The site specific concordant rates are summarized in Tables 1 and 2. Inconsistencies were found in two mutations (G12C and G13D), while others remained completely matched. No statistically significant differences were observed between the correlations of 3D-Gene[®] and Scorpion-ARMS ($\kappa = 0.97$, 95% CI 0.86 – 1.00 and 3D-Gene[®] and Luminex ($\kappa = 0.97$, 95% CI 0.86 – 1.00).

Re-analysis of discordance by Sanger sequencing

Discordant results between the three assays were identified in three cases. Discordances were observed between G12C or wild-type *KRAS* in two cases, and between G13D and wild-type *KRAS* in one case. The three discordant cases were retested using Sanger sequencing on DNA samples extracted for the 3D-Gene[®] mutation assay. A mutant allele was not detected by Sanger sequencing.

Discussion

KRAS mutation testing has become mandatory prior to the administration of therapy with the anti-EGFR antibodies, cetuximab or panitumumab, for patients with advanced colorectal cancer. *KRAS* mutation screening based on the Scorpion-ARMS *KRAS* mutation assay (therascreeen[®] *KRAS* RGQ PCR Kit, Qiagen) has been approved for *in vitro* diagnostic use in Japan. A kit using Luminex

Table 1 Detailed concordance rate between 3D-Gene[®] and Scorpion-ARMS

Mutation	MD concordance	MND concordance	Total concordance
G12A	100% (2/2)	100% (148/148)	100% (150/150)
G12C	88.3% (5/6)	99.3% (143/144)	98.6% (148/150)
G12D	100% (13/13)	100% (137/137)	100% (150/150)
G12R	100% (3/3)	100% (147/147)	100% (150/150)
G12S	100% (3/3)	100% (147/147)	100% (150/150)
G12V	100% (14/14)	100% (136/136)	100% (150/150)
G13D	92.3% (12/13)	99.3% (137/138)	99.3% (149/150)

MD: mutation detected, MND: mutation not detected.

Table 2 Detailed concordance rate between 3D-Gene[®] and Luminex

Mutation	MD concordance	MND concordance	Total concordance
G12A	100% (2/2)	100% (148/148)	100% (150/150)
G12C	100% (5/5)	99.3% (144/145)	99.3% (149/150)
G12D	100% (13/13)	100% (137/137)	100% (150/150)
G12R	100% (3/3)	100% (147/147)	100% (150/150)
G12S	100% (3/3)	100% (147/147)	100% (150/150)
G12V	100% (14/14)	100% (136/136)	100% (150/150)
G13D	100% (13/13)	100% (137/137)	100% (150/150)

MD: mutation detected, MND: mutation not detected.

(MEBGEN™ *KRAS* Mutation Detection Kit, MBL) was also approved (Fukushima et al. 2011). In this study, we examined the feasibility and robustness of the 3D-Gene[®] *KRAS* mutation assay kit.

The 3D-Gene[®] *KRAS* mutation assay kit is designed to detect 12 *KRAS* mutations on codons 12 and 13, and requires 50 ng of DNA. This assay has been validated with samples comprised of a minimum of 2.5% of tumor DNA. Thus, experimental assays demonstrate a sensitivity of 2.5%. This sensitivity is comparable to that of other methods such as Scorpion-ARMS and Luminex. We have demonstrated that the RFU values for mutant probes were remarkably lower than the respective cut-off values using HeLa DNA (wild-type *KRAS*). Based on this study, we believe that this assay provides sufficient specificity for the reliable detection of *KRAS* mutations. Estimated hands on time for Scorpion-ARMS, 3D-Gene[®], and Luminex are 2.5, 3, and 3.5 hours, respectively. Assay cost for one sample of 3D-Gene[®] and Luminex are expected to be lower than that of Scorpion-ARMS when used under the designation for “research use only”.

The correlation between the 3D-Gene[®] *KRAS* mutation assay and existing *KRAS* mutation assays is high. This result indicates that the 3D-Gene[®] mutation assay is a robust assay capable of detecting the most common clinically significant *KRAS* mutations and is comparable to existing *KRAS* mutation assays.

We detected a total of 3 discordant results among 150 (2.0%) cases in this study. The concordance rate was 98.6% between both 3D-Gene[®] and Scorpion-ARMS (148/150) and 3D-Gene[®] and Luminex (148/150). Re-analysis by Sanger sequencing could not detect any mutations. However, this might be due to tumor heterogeneity. The whole process (from DNA extraction to detection) was performed independently in each of the three assays. Differences between the methods of DNA extraction may have contributed to the discordance among the three assays.

KRAS mutations in codons 61 and 146, and *BRAF*, *NRAS*, and *PI3KCA* are also related to resistance to anti-

EGFR antibodies (Douillard et al. 2013). Therefore, further studies should be carried out to expand the use of 3D-Gene[®] technology for the detection of “all RAS” and *PI3KCA* mutations.

Conclusion

In conclusion, our results demonstrate a high concordance rate of between the 3D-Gene[®] mutation assay and the two existing *in-vitro* diagnostics kits. All three assays proved to be validated methods for detecting clinically significant *KRAS* mutations in paraffin-embedded tissue samples.

Methods

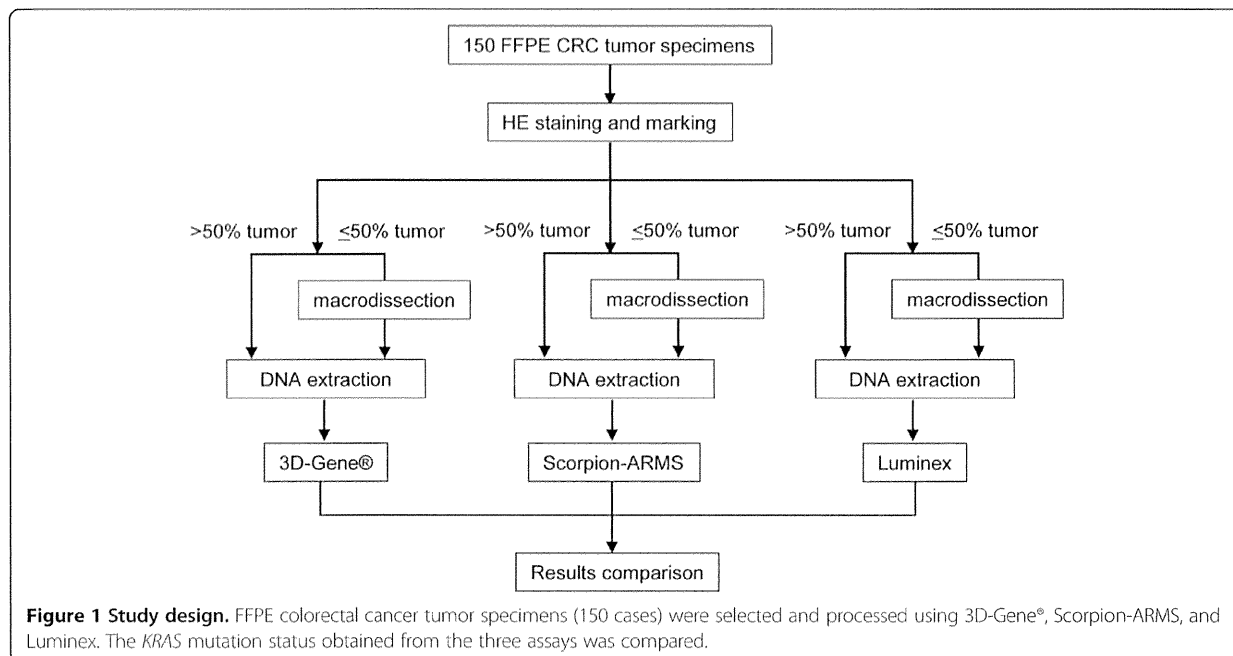
Samples

A series of 150 FFPE archived tissues was obtained from 150 Japanese patients with colorectal cancer at Kinki University Faculty of Medicine (2012–2013). All patients enrolled in the study provided written informed consent for the use of resected tissue. This study was approved by the ethics committee of Kinki University Faculty of Medicine (Authorization Number: 25–167). All samples were processed with the 3D-Gene[®] *KRAS* mutation, Scorpion-ARMS and Luminex assays. Three samples were processed with Sanger sequencing. All 150 samples were from primary colorectal carcinoma. The patient characteristics are listed in Additional file 1: Table S1.

Genomic DNA from A549, HCT-116, and HeLa cells were obtained from ATCC, Takara Bio Inc. (Shiga, Japan) and New England Biolabs Japan Inc. (Tokyo, Japan), respectively.

Study design

The study design is summarized in Figure 1. Colorectal cancer samples (150 cases) were selected by a pathologist. All of the hematoxylin and eosin-stained FFPE slides were examined and the tumor region was marked by a pathologist at Kinki University Faculty of Medicine. If the tumor region represented less than 50% on the tissue slice, the tumor regions were macrodissected. DNA extraction was performed independently for each tissue slice according to the specific standard operating procedure for each of the three assays. The 3D-Gene[®] *KRAS* mutation assay (Toray, Tokyo, Japan) was performed at the Department of Genome Biology, Kinki University (Osaka, Japan). The Scorpion-ARMS (therascreen[®] *KRAS* RGQ PCR Kit, Qiagen, Tokyo) and Luminex (MEBGEN™ *KRAS* gene mutation detection kit, MBL, Nagoya, Japan) assays were performed at the laboratories of LSI-Medience Co. (Tokyo, Japan) and SRL Inc. (Hino, Japan), respectively. All data was compiled and analyzed at Department of Genome Biology, Kinki University.

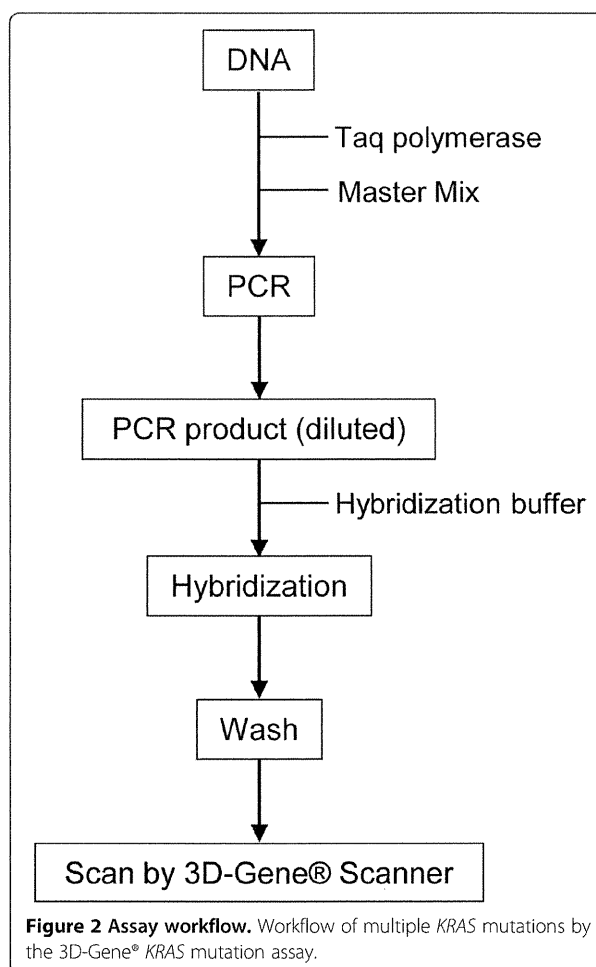


DNA extraction

Paraffin blocks were serially cut at 5 μm thickness. DNA was purified from the tissue sections using a QIAamp DNA FFPE Tissue kit (Qiagen, Valencia, CA) according to the manufacturer's instructions. DNA quantity was determined by NanoDrop spectrophotometry (NanoDrop Technologies, Wilmington, DE).

3D-Gene® mutation assay

The 3D-Gene® *KRAS* mutation assay kit (Toray, Tokyo, Japan) was used for *KRAS* mutation profiling. This kit consists of a DNA chip and PCR reagents. The DNA chip has probes to detect 12 mutations of *KRAS* codon 12 and 13 (G12S, G12C, G12R, G12D, G12V, G12A, G13S, G13C, G13R, G13D, G13V and G13A). The cutoff value for determining positive mutations was set to 300, but G12C and G13C were set 385 and 537, respectively. Fifty nanograms of DNA derived from FFPE tissue was amplified with the supplied reagent. The PCR product labeled with fluorescent dye was hybridized onto the DNA chip surface after denaturation at 95°C for 2 min. Chips were incubated at 59°C for 30 min under agitation at 1,400 rpm. After hybridization, the DNA chips were washed and dried in an ozone-free environment. The fluorescent image was scanned with the 3D-Gene® Scanner 3000 (Toray Industries, Inc.). The images obtained from the DNA chip were quantified by measuring the relative fluorescence unit (RFU) using 3D-Gene® ExTraction software (Toray Industries, Inc.). This assay determined the mutation to be positive if signal detected was greater than the cutoff value. The assay workflow is illustrated in Figure 2. Probe arrangements in



a cell and representative scanned image of a microarray are shown in Additional file 2: Figures S1 and S2, respectively. Cutoff values were established using *KRAS* wild-type and mutant plasmid DNA. We set the average + 5SD (RFU) values obtained from the *KRAS* wild-type plasmid DNA as tentative cutoff value. The values for the mutation sites were 385, 537, and 300 RFU for G12C, G13C, and others, respectively. When the 3D-Gene[®] assay was performed using codon 12 mutant plasmid DNA, the minimum measured value among codon 12 mutation was 1009 RFU (G12R), whereas all codon 13 mutation values were below 300 RFU. When the 3D-Gene[®] assay was performed using codon 13 mutant plasmid DNA, the minimum measured value among codon 13 mutation was 332 RFU (G13S), whereas all codon 12 mutation values were below 300 RFU. All assays were performed eight times independently. Based on these data, we set the cutoff values for G12C, G13C, and others at 385, 537, and 300 RFU, respectively. Similarly, the cutoff value for wild-type was set to 300 RFU.

Sensitivity assay

The sensitivity of the 3D-Gene[®] mutation assay was evaluated by mixing G12S (codon 12) or G13D (codon 13) mutated and wild-type DNA from cell lines (A549 as codon 12 mutated, HCT-116 codon 13 and HeLa cells as wild-type, respectively) at 100%, 50%, 25%, 5%, 2.5% and 1% ratios.

Scorpion-ARMS

The Scorpion-ARMS assay was analyzed using the therascreen[®] *KRAS* RGQ PCR Kit (Qiagen). The Scorpion-ARMS assay is a real time-PCR assay that combines the Amplification Refractory Mutation System (ARMS) and Scorpions fluorescent primer/probe system. This assay detects G12S, G12C, G12R, G12D, G12V, G12A, and G13D mutations of *KRAS*. The sensitivity is 1%. This assay was performed according to the manufacturer's guidelines (Qiagen). Briefly, DNA was isolated from FFPE tissue samples and the total sample DNA assessed by amplifying a region of exon 2 from *KRAS* by PCR. Next, the DNA samples were tested for the presence or absence of *KRAS* mutations by real-time PCR using a Scorpion probe and primers specific for wild-type and mutant *KRAS* DNA. The differences between the mutation assay cycle threshold (C_y) values were determined. Samples were designated mutation positive if the δC_y was less than the cutoff δC_y value.

Luminex

The Luminex assay was analyzed using the MEBGEN[™] *KRAS* kit (MBL, Nagoya, Japan), which is currently approved for clinical use by the Ministry of Health, Labour and Welfare of Japan (Fukushima et al. 2011). The Luminex assay is based on PCR-rSSO method (Itoh et al. 2005); First,

50 ng of template DNA collected from FFPE tissue samples was amplified by PCR using a biotin-labeled primer. Thereafter, the PCR products and fluorescent Luminex beads (oligonucleotide probes complementary to wild and mutant genes bound to the beads) were hybridized and labeled with streptavidin-phycoerythrin. Subsequently, the products were processed by the Luminex assay and the data collected was then analyzed using UniMAG software (MBL, Japan). This assay detects G12S, G12C, G12R, G12D, G12V, G12A, G13S, G13C, G13R, G13D, G13V and G13A mutations of *KRAS*.

Sequencing analysis

DNA samples obtained from specimens that were discordant between three assays were amplified using the following site-specific primers: forward 5' -AAGGCCTGC TGAAAATGACTG- 3', reverse 5' -GTCCTGCACCAG TAATATGC- 3'. The purified products were sequenced using BigDye terminator v3.1 (Applied Biosystems, Foster City, CA) with ABI 3100 Genetic Analyzer (Applied Biosystems).

Statistics

Kappa statistics were used to compare the 3D-Gene[®] *KRAS* mutation assay with the Scorpion-ARMS and Luminex assays.

Additional files

Additional file 1: Table S1. Clinicopathological characteristics primary colorectal cancer patients providing FFPE samples. **Table S2.** Results of three different assay. **Table S3.** Methods correlation between 3D-Gene[®] and Scorpion-ARMS. **Table S4.** Methods correlation between 3D-Gene[®] and Luminex.

Additional file 2: Figure S1. Probe arrangements in a microarray cell. The microarray slide is divided into 8 compartments. Each cell has 13 probes of the *KRAS* gene, and each probe is represented six times on the slide. WT: wild-type *KRAS*, NC: negative control. **Figure S2.** Representative scanned image of a microarray. Images shown are representative of images from three mutant (G12C, G12S and G13D), three wild-type (WT), one WT control and one negative control (distilled water) samples.

Competing interests

Akihiko Ito and Kazuto Nishio (Kinki University) have received funding from Toray Industries, Inc. Yoji Ueda, Satoshi Kondo and Hitoshi Nobumasa are full-time employees of Toray Industries, Inc. No potential conflicts of interest were disclosed by the other authors.

Authors' contributions

KS carried out the mutation analysis. AZ and AI collected clinical samples and pathological data. YU, SK, and HN carried out the sensitivity assay. YF, YT, and MT participated in the study design. MV and ST carried out the data analysis. KN conceived of the study and wrote the manuscript. All authors read and approved the final manuscript.

Acknowledgements

We thank Y Hosono, T Kitayama, and A Kurumatani for technical assistance.

Funding information

This study was sponsored by Toray Industries, Inc. This means that the publication of this study is written by investigators and has no relative value of the 3D-Gene® KRAS mutation assay for the promotion.

Author details

¹Department of Genome Biology, Kinki University Faculty of Medicine, Osaka-Sayama, Osaka, Japan. ²Department of Pathology, Kinki University Faculty of Medicine, Osaka-Sayama, Osaka, Japan. ³New Projects Development Division, Toray Industries, Inc., Kamakura, Kanagawa, Japan.

Received: 23 October 2014 Accepted: 16 December 2014

Published: 5 January 2015

References

- Allegra CJ, Jessup JM, Somerfield MR, Hamilton SR, Hammond EH, Hayes DF, McAllister PK, Morton RF, Schilsky RL (2009) American Society of Clinical Oncology provisional clinical opinion: testing for KRAS gene mutations in patients with metastatic colorectal carcinoma to predict response to anti-epidermal growth factor receptor monoclonal antibody therapy. *J Clin Oncol* 27:2091–2096
- Altimari A, de Biase D, De Maglio G, Gruppioni E, Capizzi E, Degiovanni A, D'Errico A, Pession A, Pizzolitto S, Fiorentino M, Tallini G (2013) 454 next generation-sequencing outperforms allele-specific PCR, Sanger sequencing, and pyrosequencing for routine KRAS mutation analysis of formalin-fixed, paraffin-embedded samples. *Onco Targets Ther* 6:1057–1064
- Amado RG, Wolf M, Peeters M, Van Cutsem E, Siena S, Freeman DJ, Juan T, Sikorski R, Suggs S, Radinsky R, Patterson SD, Chang DD (2008) Wild-type KRAS is required for panitumumab efficacy in patients with metastatic colorectal cancer. *J Clin Oncol* 26:1626–1634
- Andreyev HJ, Norman AR, Cunningham D, Oates JR, Clarke PA (1998) Kirsten ras mutations in patients with colorectal cancer: the multicenter "RASCAL" study. *J Natl Cancer Inst* 90:675–684
- Bokemeyer C, Bondarenko I, Hartmann JT, de Braud F, Schuch G, Zubel A, Celik I, Schlichting M, Koralewski P (2011) Efficacy according to biomarker status of cetuximab plus FOLFFOX-4 as first-line treatment for metastatic colorectal cancer: the OPUS study. *Ann Oncol* 22:1535–1546
- Bokemeyer C, Van Cutsem E, Rougier P, Ciardiello F, Heeger S, Schlichting M, Celik I, Köhne CH (2012) Addition of cetuximab to chemotherapy as first-line treatment for KRAS wild-type metastatic colorectal cancer: pooled analysis of the CRYSTAL and OPUS randomised clinical trials. *Eur J Cancer* 48:1466–1475
- Chang SC, Denne J, Zhao L, Horak C, Green G, Khambata-Ford S, Bray C, Celik I, Van Cutsem E, Harbison C (2013) Comparison of KRAS genotype: theascreen assay vs. LNA-mediated qPCR clamping assay. *Clin Colorectal Cancer* 2:195–203
- De Roock W, Piessevaux H, De Schutter J, Janssens M, De Hertogh G, Personeni N, Biesmans B, Van Laethem JL, Peeters M, Humblet Y, Van Cutsem E, Tejpar S (2008) KRAS wild-type state predicts survival and is associated to early radiological response in metastatic colorectal cancer treated with cetuximab. *Ann Oncol* 19:508–515
- Douillard JY, Oliner KS, Siena S, Tabernero J, Burkes R, Barugel M, Humblet Y, Bodoky G, Cunningham D, Jassem J, Rivera F, Kocáková I, Ruff P, Blasińska-Morawiec M, Šmakal M, Canon JL, Rother M, Williams R, Rong A, Wizeorek J, Sidhu R, Patterson SD (2013) Panitumumab-FOLFFOX4 treatment and RAS mutations in colorectal cancer. *N Engl J Med* 369:1023–1034
- Fukushima Y, Yanaka S, Murakami K, Abe Y, Koshizaka T, Hara H, Samejima C, Kishi Y, Kaneda M, Yoshino T (2011) High-throughput screening method of KRAS mutations at codons 12 and 13 in formalin-fixed paraffin-embedded tissue specimens of metastatic colorectal cancer. *Gan To Kagaku Ryoho* 38:1825–1835
- Gonzalez de Castro D, Angulo B, Gomez B, Mair D, Martinez R, Suarez-Gauthier A, Shieh F, Velez M, Brophy VH, Lawrence HJ, Lopez-Rios F (2012) A comparison of three methods for detecting KRAS mutations in formalin-fixed colorectal cancer specimens. *Br J Cancer* 107:345–351
- Harlé A, Busser B, Rouyer M, Harter V, Genin P, Leroux A, Merlin JL (2013) Comparison of COBAS 4800 KRAS, TaqMan PCR and high resolution melting PCR assays for the detection of KRAS somatic mutations in formalin-fixed paraffin embedded colorectal carcinomas. *Virchows Arch* 462:329–335
- Itoh Y, Mizuki N, Shimada T, Azuma F, Itakura M, Kashiwase K, Kikkawa E, Kulski JK, Satake M, Inoko H (2005) High-throughput DNA typing of HLA-A, -B, -C, and -DRB1 loci by a PCR-SSOP-Luminex method in the Japanese population. *Immunogenetics* 57:717–729

- Jonker DJ, O'Callaghan CJ, Karapetis CS, Zalberg JR, Tu D, Au HJ, Berry SR, Krahn M, Price T, Simes RJ, Tebbutt NC, van Hazel G, Wierzbicki R, Langer C, Moore MJ (2007) Cetuximab for the treatment of colorectal cancer. *N Engl J Med* 357:2040–2048
- Karapetis CS, Khambata-Ford S, Jonker DJ, O'Callaghan CJ, Tu D, Tebbutt NC, Simes RJ, Chalchal H, Shapiro JD, Robitaille S, Price TJ, Shepherd L, Au HJ, Langer C, Moore MJ, Zalberg JR (2008) K-ras mutations and benefit from cetuximab in advanced colorectal cancer. *N Engl J Med* 359:1757–1765
- Lièvre A, Bachet JB, Le Corre D, Boige V, Landi B, Emile JF, Côté JF, Tomasic G, Penna C, Ducreux M, Rougier P, Penault-Llorca F, Laurent-Puig P (2006) KRAS mutation status is predictive of response to cetuximab therapy in colorectal cancer. *Cancer Res* 66:3992–3995
- Lièvre A, Bachet JB, Boige V, Cayre A, Le Corre D, Buc E, Ychou M, Bouché O, Landi B, Louvet C, André T, Bibeau F, Diebold MD, Rougier P, Ducreux M, Tomasic G, Emile JF, Penault-Llorca F, Laurent-Puig P (2008) KRAS mutations as an independent prognostic factor in patients with advanced colorectal cancer treated with cetuximab. *J Clin Oncol* 26:374–379
- Sato F, Tsuchiya S, Terasawa K, Tsujimoto G (2009) Intra-platform repeatability and inter-platform comparability of microRNA microarray technology. *PLoS One* 4:e5540
- Sudo H, Mizoguchi A, Kawauchi J, Akiyama H, Takizawa S (2012) Use of non-amplified RNA samples for microarray analysis of gene expression. *PLoS One* 7:e31397
- Van Cutsem E, Köhne CH, Láng I, Folprecht G, Nowacki MP, Cascinu S, Shchepotin I, Maurel J, Cunningham D, Tejpar S, Schlichting M, Zubel A, Celik I, Rougier P, Ciardiello F (2011) Cetuximab plus irinotecan, fluorouracil, and leucovorin as first-line treatment for metastatic colorectal cancer: updated analysis of overall survival according to tumor KRAS and BRAF mutation status. *J Clin Oncol* 29:2011–2019

doi:10.1186/2193-1801-4-7

Cite this article as: Sakai et al.: Performance of a novel KRAS mutation assay for formalin-fixed paraffin embedded tissues of colorectal cancer. *SpringerPlus* 2015 4:7.

Submit your manuscript to a SpringerOpen® journal and benefit from:

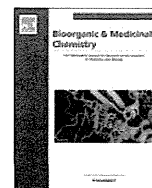
- Convenient online submission
- Rigorous peer review
- Immediate publication on acceptance
- Open access: articles freely available online
- High visibility within the field
- Retaining the copyright to your article

Submit your next manuscript at ► springeropen.com



Contents lists available at ScienceDirect

Bioorganic & Medicinal Chemistry

journal homepage: www.elsevier.com/locate/bmc

Design, synthesis, and structure–activity relationships of 1-ethylpyrazole-3-carboxamide compounds as novel hypoxia-inducible factor (HIF)-1 inhibitors

Yorinobu Yasuda^a, Takeaki Arakawa^a, Yumi Nawata^a, Sayaka Shimada^a, Shinya Oishi^b, Nobutaka Fujii^b, Shinichi Nishimura^a, Akira Hattori^a, Hideaki Kakeya^{a,*}

^a Department of System Chemotherapy and Molecular Sciences, Division of Bioinformatics and Chemical Genomics, Graduate School of Pharmaceutical Sciences, Kyoto University, Sakyo-ku, Kyoto 606-8501, Japan

^b Department of Bioorganic Medicinal Chemistry & Chemogenomics, Division of Bioinformatics and Chemical Genomics, Graduate School of Pharmaceutical Sciences, Kyoto University, Sakyo-ku, Kyoto 606-8501, Japan

ARTICLE INFO

Article history:

Received 27 December 2014

Revised 14 February 2015

Accepted 17 February 2015

Available online xxx

Keywords:

Hypoxia-inducible factor (HIF)

Cancer

Chemotherapy

Structure–activity relationship

ABSTRACT

Hypoxia-inducible factor (HIF)-1 is well known as a promising target for cancer chemotherapy. By screening an in-house chemical library using a hypoxia-responsive luciferase reporter gene assay, we identified CLB-016 (**1**) containing 1-ethylpyrazole-3-carboxamide as a HIF-1 inhibitor (IC₅₀ = 19.1 μM). In a subsequent extensive structure-activity relationship (SAR) study, we developed compound **11Ae** with an IC₅₀ value of 8.1 μM against HIF-1-driven luciferase activity. Compounds **1** and **11Ae** were shown to significantly suppress the HIF-1-mediated hypoxia response, including carbonic anhydrase IX (CAIX) gene expression and migration of human sarcoma HT1080 cells. These results revealed 1-ethylpyrazole-3-carboxamide as a novel scaffold to develop promising anti-cancer drugs targeting the HIF-1 signaling pathway.

© 2015 Elsevier Ltd. All rights reserved.

1. Introduction

Tumor cells survive in harsh conditions, such as hypoxia and exposure to poor nutrition by changing their metabolic pathway.¹ Hypoxia-inducible factor (HIF)-1, a basic helix–loop–helix transcriptional factor, promotes the transcription of a number of genes involved in cellular adaptive responses to low availability of oxygen and nutrients, such as glucose transporter-1 (*GLUT*), vascular endothelial growth factor (*VEGF*) and carbonic anhydrase IX (*CAIX*).² Therefore, it has been proposed that HIF-1 is a promising molecular target for cancer chemotherapy.

To date, dozens of compounds have been reported to suppress the HIF-1 signaling pathway (Fig. 1).^{3,4} For example, YC-1, the most-widely used HIF-1 inhibitor, suppresses HIF-1-mediated

transcription through the promotion of hydroxylation at Asn-803 of HIF-1α by factor-inhibiting-HIF (FIH), which, in turn, disrupts the association of its C-terminal transactivation domain with p300/CBP, a critical co-factor of HIF-1.⁵ The inhibition of HIF-1 activity by YC-1 suppresses tumor metastasis and decreases the incidence of post-irradiation tumor recurrence.⁶

To generate new inhibitors against HIF-1, we screened an in-house chemical library using a hypoxia-responsive luciferase reporter gene assay. We here report CLB-016 (**1**) with 1-ethyl pyrazole-3-carboxamide as a potent inhibitor. Through an extensive structure–activity relationship (SAR) study of CLB-016 (**1**), we have successfully developed more potent HIF-1 inhibitors.

2. Results and discussion

2.1. Discovery of CLB-016 (**1**)

To identify novel HIF-1 inhibitors, we screened an in-house chemical library using a hypoxia-response element (HRE)-driven luciferase assay system. Human fibrosarcoma HT1080 cells with stably-integrated x5HRE-luciferase reporter were treated with the tested compounds at 100 μM under hypoxic conditions (1%

Abbreviations: HIF-1, hypoxia-inducible factor-1; CA, carbonic anhydrase; FIH, factor-inhibiting-HIF; SAR, structure–activity relationship; SEM, 2-(trimethylsilyl)ethoxymethyl; HRE, hypoxia-response element; VEGF, vascular endothelial growth factor; TBAI, tetrabutylammonium iodide; HATU, 1-(bis(dimethylamino)methylene)-1H-1,2,3-triazolo(4,5-b)pyridinium 3-oxide hexafluorophosphate.

* Corresponding author. Tel.: +81 75 753 4524; fax: +81 75 753 4591.

E-mail address: sceigygo-hisyo@pharm.kyoto-u.ac.jp (H. Kakeya).

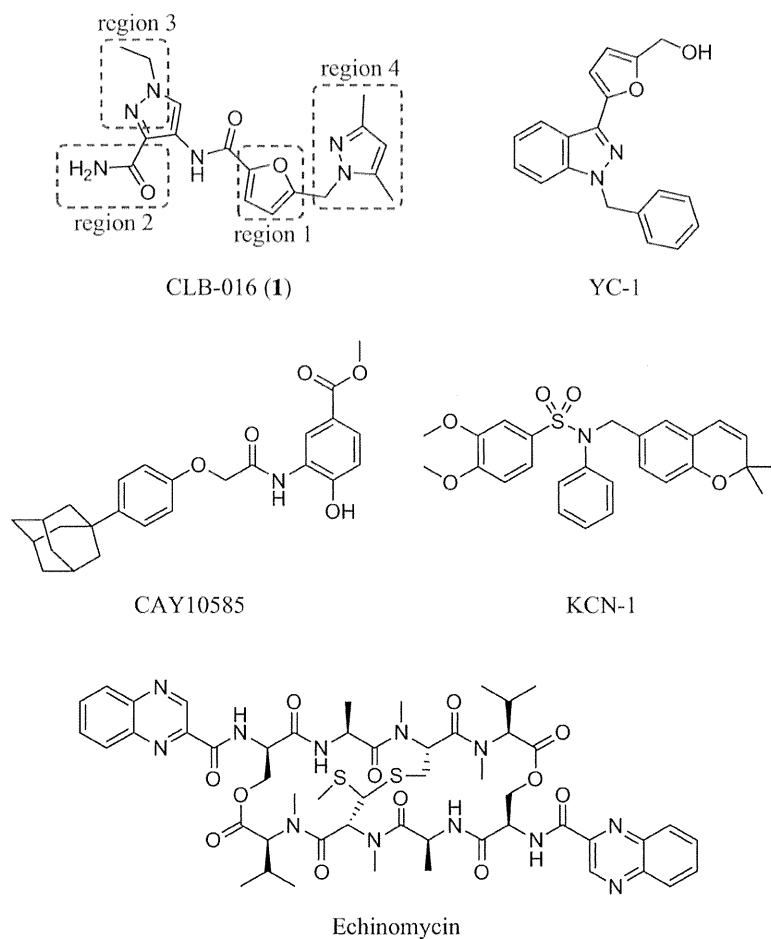


Figure 1. Chemical structures of CLB-016 (1) and representative HIF-1 inhibitors.

O₂) for 24 h. Among approximately 6000 compounds, CLB-016 (1, Fig. 1) significantly decreased hypoxia-induced luciferase activity (89.8% inhibition compared with vehicle control). Interestingly, CLB-016 (1) exhibited a novel chemotype among various HIF-1 inhibitors,^{3,4} which promoted us to undertake a SAR study of this compound.

2.2. Design and synthesis of CLB-016 (1) and its derivatives

We planned to synthesize analogues by conjugation of 4-amino-pyrazole (left segment), pyrazole (right segment), and the remaining middle segment (Fig. 1). The furan ring in the middle segment was replaced by other aromatic rings (region 1). Next, substitutions of the left-pyrazole ring were investigated (regions 2 and 3). Then, the size and lipophilicity of the right-pyrazole ring were examined (region 4).

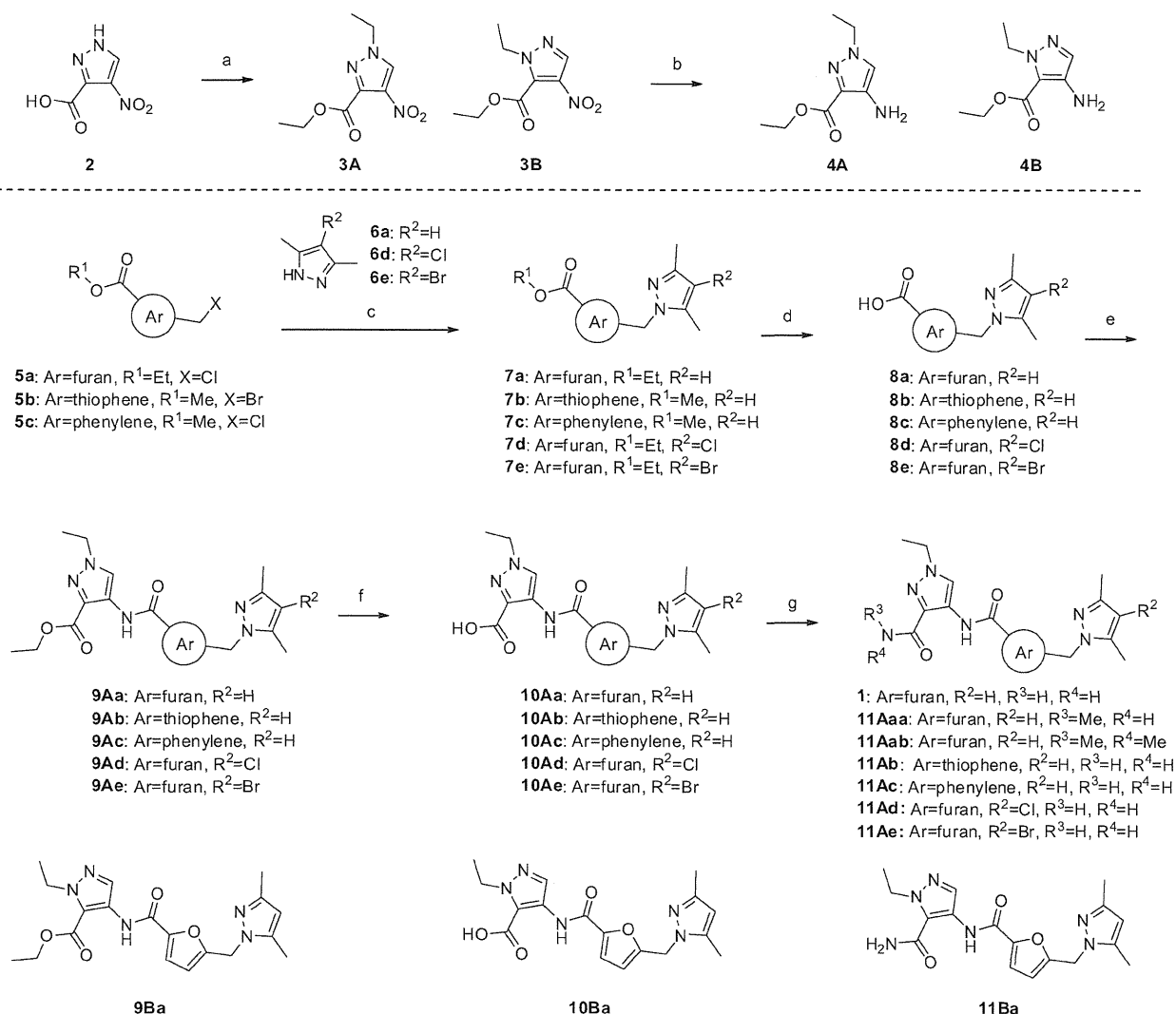
The synthetic route of 1-ethylpyrazole-3-carboxamide is shown in Scheme 1. The left segments were first synthesized. Commercially available 4-nitro-1*H*-pyrazole-3-carboxylic acid (2) was alkylated with excess ethyl iodide in the presence of potassium carbonate in DMF. After flash chromatography on silica gel, two regioisomers, ethyl 1-ethyl-4-nitro-1*H*-pyrazole-3-carboxylate (3A, 1,3-isomer) and ethyl 1-ethyl-4-nitro-1*H*-pyrazole-5-carboxylate (3B, 1,5-isomer) were obtained in 34.4% and 20.7% yield, respectively. This regioselectivity might be due to a steric hindrance of both the ethyl group and the carboxyl group at pyrazole 3-position. The nitro group of 3A and 3B was reduced by

hydrogenation in the presence of a catalytic amount of 10% Pd/C to produce amines 4A and 4B, respectively. The structures of the isomers (4A, 4B) were determined by NOESY analysis: a NOESY correlation was observed between H-5 and ethyl protons in 4A.

Next, dimethyl pyrazole (6), the right segment, was reacted with various substituted benzyl halides, and heteroarylmethyl halides (5a–5c) in the presence of KOtBu to yield the corresponding alkyl 4-substituted aryl or heteroaryl-2-carboxylates (7a–7e). The ester compounds 7a–7e were hydrolyzed with NaOH to generate carboxylic acids (8a–8e). These carboxylic acids were condensed with aminopyrazole 4A or 4B to yield the corresponding amides (9Aa–9Ae, 9Ba). Hydrolysis of the ester group with NaOH gave the corresponding acids, followed by their conversion into the amide compounds (1, 11Aaa–11Ae, 11Ba).

Compound 18 lacking an ethyl group in CLB-016 (1) was synthesized in a similar fashion to CLB-016 (1) (Scheme 2). 4-Nitro-1*H*-pyrazole-3-carboxylic acid (2) was first converted to the methyl ester 12, followed by protection with 2-(trimethylsilyl)ethoxymethyl (SEM) group to afford 13, which could be separated from the 1,5-isomer by silica gel flash chromatography. The nitro compound 13 was reduced and conjugated with the middle-right part 8a. The obtained methyl ester 15 was hydrolyzed, converted to carboxamide 17, and finally deprotected to yield the target compound 18.

We designed the other compound 23 to test the importance of the carboxamide in the left segment. Synthesis was commenced



Scheme 1. Synthesis of CLB-016 (**1**) and its derivatives. Reagents and conditions: (a) ethyl iodide, K₂CO₃, DMF, rt; (b) Pd/C, H₂, EtOH, rt; (c) **6a/6d/6e**, KOtBu, TBAI, THF, rt; (d) 5 N NaOH aq, EtOH, rt; (e) **4A/4B**, HATU, Hunig's base, DMF, MW 50 °C; (f) 5 N NaOH aq, EtOH, rt; (g) R₃R₄NH, HATU, Hunig's base, DMF, rt or MW 50 °C.

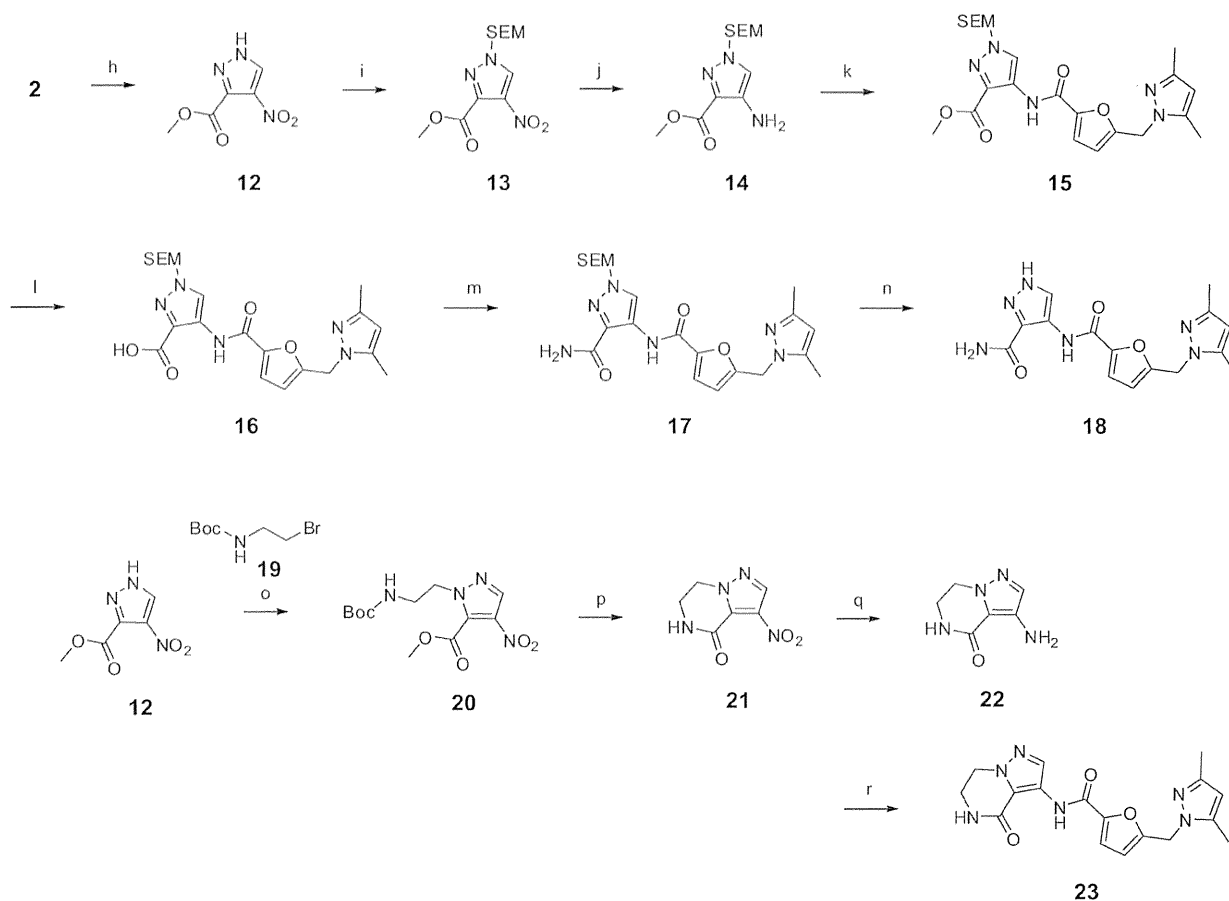
by alkylation of the methyl ester **12** with *tert*-butyl 2-bromoethylcarbamate (**19**) to obtain methyl 1-(2-(*tert*-butoxycarbonylamino)ethyl)-4-nitro-1H-pyrazole-5-carboxylate **20** (Scheme 2). As in the case of alkylation from **2** to **3**, the desired 1,5-isomer **20** was separated from the 1,3-isomer by silica gel flash chromatography. The Boc group in **20** was removed in an acidic condition, and the resulting primary amine in an HCl salt form was reacted with the methyl ester to give the cyclic amide **21** in a basic condition. The nitro group in **21** was reduced by hydrogenation to give an amine **22**. Finally, condensation of **22** with **8a** furnished the target compound **23**.

2.3. Biological activities

HIF-1 inhibitory activity of the synthesized analogues was examined in HT1080 cells stably-expressing x5HRE-luciferase reporter. In our system, YC-1, a HIF-1 inhibitor, exhibited marginal inhibitory activity with an IC₅₀ value of 48.4 μM. This compound inhibited proliferation of cells cultured under hypoxia with an IC₅₀ value of 30.9 μM. In contrast, CLB-016 (**1**) (IC₅₀ = 19.1 μM) inhibited the HIF-1 signaling pathway in a dose-dependent manner (Fig. 2A). As shown in Table 1, replacement of the furan ring of **1** with thiophene (**11Ab**) or benzene (**11Ac**) caused a substantial

decrease in the HIF-1 inhibitory activity (IC₅₀: >100 and 72.0 μM, respectively). This could be attributed to the difference in the bond angle of bisection among furan (C–O–C), thiophene (C–S–C), and 1,3-disubstituted benzene (C1–C2–C3). Thus, the species of the central ring determined the overall molecular conformation, which consequently affected the HIF-1 inhibitory activity.^{7,8} It is alternatively conceivable that a heteroatom in the central ring plays an important role in its interaction with target molecule(s).

We could modulate potency by changing the substitution pattern of the carboxamide group. Non-methylated amide **1** and mono-methylated amide **11Aaa** exhibited equipotent HIF-1 inhibitory activity, while dimethylated amide **11Aab** exhibited decreased potency both in the HIF-1 inhibitory activity and in the anti-proliferative activity against HT1080 cells. Since the ¹H NMR signals of the two carboxamide protons in compound **1** were not equivalent (δ_H 6.74 and 5.62 ppm), there may exist a five-membered ring formed by intramolecular hydrogen bonding between the carboxamide proton and the pyrazole nitrogen. This five-membered ring can fix the direction of the carbonyl oxygen atom, which might be prerequisite for its activity. In contrast, compound **11Aab** cannot fix the conformation of carboxamide, as this compound has no proton atom on the nitrogen. We also



Scheme 2. Synthesis of **18** and **23**. Reagents and conditions: (h) Acetyl chloride, MeOH, rt; (i) SEM-Cl, NaH, THF, rt; (j) H₂, Pd/C, 40 °C; (k) **8a**, HATU, Hunig's base, DMF, MW 50 °C; (l) 5 N NaOH aq, EtOH, rt; (m) NH₄Cl, HATU, Hunig's base, DMF, MW 50 °C; (n) 2 M HCl/EtOH, MW 80 °C; (o) **19**, K₂CO₃, TBAI, DMF, rt; (p) 2 M HCl/EtOH, 50 °C; (ii) Hunig's base, toluene, 100 °C; (q) Pd/C, H₂, EtOH, 40 °C; (r) **8a**, HATU, Hunig's base, DMF, MW 50 °C.

investigated the effect of the alkyl chain in the left pyrazole ring. The ethyl group in CLB-016 (**1**) was indispensable for the HIF-1 inhibitory activity, because compound **18** with no alkylation showed only marginal inhibition compared with CLB-016 (**1**). In addition, the effect of compound **11Ba**, a regioisomer of **1**, on both the reporter activity and proliferation of HT1080 cells was found to be negligible. Thus, it is suggested that both formation of the intramolecular hydrogen bond and proper substitution of an ethyl group in the pyrazole ring are indispensable for the potent HIF-1 inhibitory activity. This was also supported by the invalidity of compound **23** with 6,7-dihydropyrazolopyrazinone containing a six-membered cyclic amide.

We next investigated the effect of the size and lipophilicity of the right pyrazole ring on the HIF-1 inhibitory activity. As shown in Table 2, the importance of the dimethyl substitution was demonstrated by compound **24**, which had no methyl group and exhibited marginal HIF-1 inhibitory activity (IC₅₀ = 81.8 μM). Furthermore, compound **25** with dimethylisoxazole lost its inhibitory activity (IC₅₀ > 100 μM), suggesting the importance of the lipophilic surfaces of the molecule for its activity. In fact, introduction of a halogen atom at position 4 of dimethyl pyrazole furnished much more potent inhibitors, for example, **11Ad** (Cl, HRE-Luc IC₅₀ = 8.7 μM) and **11Ae** (Br, HRE-Luc IC₅₀ = 8.1 μM). Alternatively, it is also plausible that an increase in the lipophilicity of the molecules contributed to the elevation of their biological activities by increasing the permeability of the plasma membrane⁹: each *A*Log*P* for **1**, **11Ad**, and **11Ae** is 1.18, 1.84, and 1.93, respectively.

We evaluated the inhibitory activities of CLB-016 (**1**) and its derivatives toward HIF-1 transcriptional activity by measuring the endogenous mRNA levels of *CAIX* gene, a HIF-1 target gene. As shown in Figure 2B, the *CAIX* gene in HT1080 cells was actively transcribed under hypoxia (153-fold over normoxia). Quantitative RT-PCR analysis demonstrated that compound **1** significantly suppressed the hypoxia-induced *CAIX* expression with comparable dose-dependency to its HRE-luc inhibition. In contrast, CLB-016 (**1**) did not affect the mRNA levels of *HIF-1α* and *-1β* up to 100 μM, suggesting that the inhibition of hypoxia-induced responses, such as elevation of luciferase activity and *CAIX* mRNA expression, by the compound was not due to general inhibition of transcription. As shown in Figure 2C, CLB-016 derivatives (**11Ad** and **11Ae**, but not **11Ba**) decreased the hypoxia-induced *CAIX* mRNA levels with good correlation to their HRE-reporter inhibition. Finally, these active compounds including **1**, **11Ad** and **11Ae**, were found to significantly suppress the motility of HT1080 cells (Fig. 3), which is known to be facilitated by several HIF-1-regulated genes including *VEGF* and *CAIX*.¹⁰ Taken together, it is conceivable that a series of 1-ethylpyrazole-3-carboxamide compounds are able to modulate cellular adaptive responses to hypoxia by specifically inhibiting the HIF-1 signaling pathway.

3. Conclusions

In the current study, we identified CLB-016 (**1**) and developed its derivatives containing 1-ethylpyrazole-3-carboxamide as

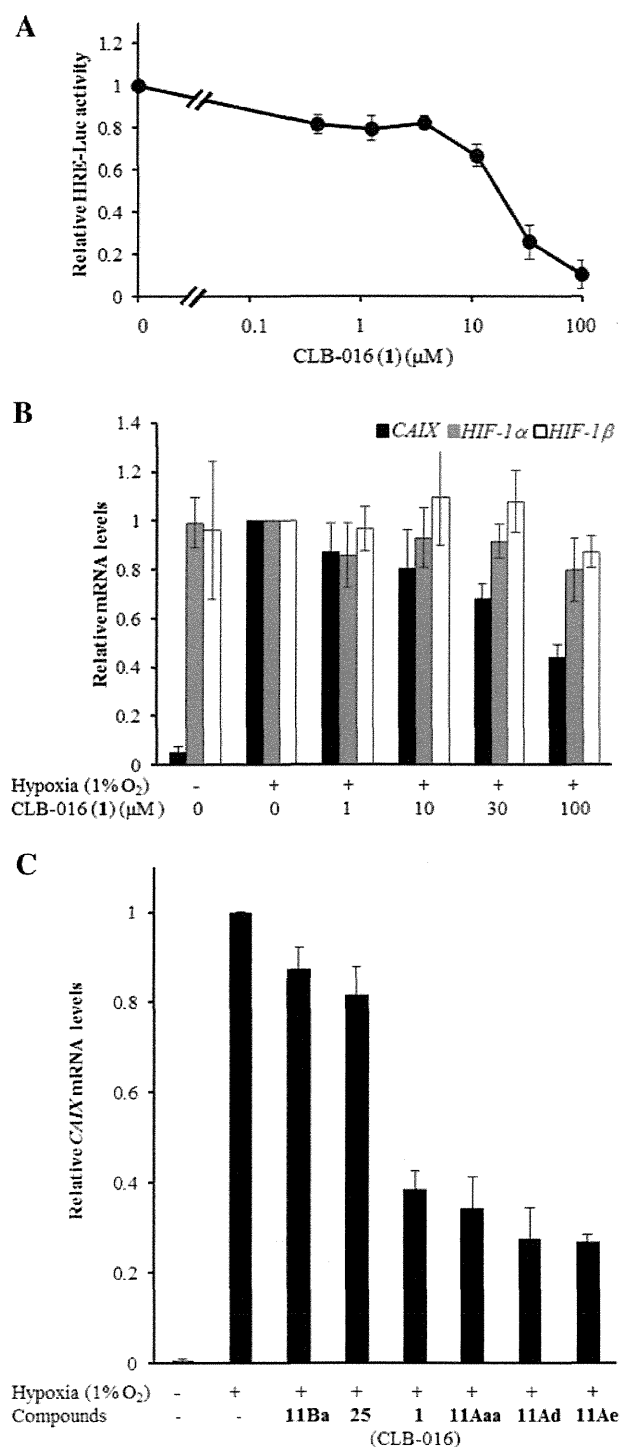


Figure 2. Inhibition of HIF-1-mediated transcription by CLB-016 (**1**) and its derivatives. (A) Dose-dependent inhibition of hypoxia-induced luciferase activity by CLB-016 (**1**). x5HRE/HT1080 cells were incubated with the compound for 24 h under hypoxia (1% O₂). The luciferase activity of CLB-016 (**1**)-treated cells relative to that of DMSO-treated cells are shown. (B) Effects of CLB-016 (**1**) on the expression of the human *CAIX*, *HIF-1 α* , and *HIF-1 β* genes. Cells were treated with the compound for 4 h. mRNA levels were quantified by real-time PCR, normalized to 18S rRNA levels, and presented as relative values against that of DMSO-treated cells. (C) Effects of CLB-016 (**1**) and its derivatives against the mRNA levels of *CAIX*. Cells were treated with compounds at 100 μM for 16 h. mRNA levels were measured by quantitative PCR analysis as in (B), and the values relative to that under normoxic conditions are shown. Data represent the mean \pm standard error ($n = 3$).

HIF-1 inhibitors. SAR studies revealed that: (1) 1-ethylpyrazole-3-carboxamide moiety (regions 2 and 3) required both protons on the carboxamide group and proper substitution of an ethyl group for HIF-1 inhibitory activity; (2) investigation of the central ring (region 1) suggested the importance of the bond angle of the bisection among the hetero-aromatic ring for activity; and (3) introduction of a halogen atom on the right pyrazole ring (region 4) improved activity. Because CLB-016 derivatives possess drug-like physicochemical properties (molecular weight of 100–350, LogP value of 1–3),¹¹ 1-ethylpyrazole-3-carboxamide compounds are promising lead compounds from which to develop novel anti-cancer drugs targeting the HIF-1 signaling pathway. Although we have not identified the target molecule(s) of the compounds, we demonstrated that CLB-016 (**1**) and its derivatives should affect the HIF-1-dependent pathway. Detailed studies of the mechanism of action of 1-ethylpyrazole-3-carboxamide compounds on HIF-1 signaling are required, and are currently being undertaken in our laboratory.

4. Experimental section

4.1. Chemistry

Reactions in microwave reactors were performed by single-node heating in an Initiator (Biotage). Flash column chromatography was performed manually or by using a Biotage SP-1 Flash. High-resolution mass spectra were measured on LC-IT-TOF MS (Shimadzu) mass spectrometers. The ¹H NMR (400 MHz) and ¹³C NMR (100 MHz) spectra were recorded on JEOL AL-400 and JEOL ECS-400 with tetramethylsilane as an internal standard. Abbreviations are as follows: s, singlet; d, doublet; t, triplet; q, quartet; m, multiplet; br, broad. Melting points were measured by BÜCHI Melting Point B-545 (BÜCHI Labortechnik AG). IR spectra were measured on a SHIMADZU FTIR-8400S spectrometer. Compounds **25** and **YC-1** were purchased from Princeton BioMolecular Research, Inc. and Santa Cruz Biotechnology, Inc., respectively.

4.1.1. Ethyl 1-ethyl-4-nitro-1H-pyrazole-3-carboxylate (**3A**) and ethyl 1-ethyl-4-nitro-1H-pyrazole-5-carboxylate (**3B**)

4-Nitro-1H-pyrazole-3-carboxylic acid (**1**) (300 mg, 1.91 mmol) was added to a stirred solution of ethyl iodide (324 μl , 4.01 mmol) and K₂CO₃ (660 mg, 4.77 mmol) in DMF (9 ml). The reaction mixture was stirred at rt for 3 h, and then the mixture was filtrated and concentrated. The residue was suspended in H₂O and extracted with EtOAc. The organic layer was washed with H₂O and brine, dried over Na₂SO₄, and concentrated in vacuo. The residue was purified by silica gel column chromatography (hexane/EtOAc) to give **3A** (140 mg, 0.656 mmol, 34.4%) as a pale brown oil and **3B** (84 mg, 0.395 mmol, 20.7%) as a pale brown oil.

Compound **3A**: ¹H NMR (CDCl₃) δ 8.16 (s, 1H), 4.47 (q, $J = 7.2$ Hz, 2H), 4.26 (q, $J = 7.3$ Hz, 2H), 1.57 (t, $J = 7.3$ Hz, 3H), 1.41 (t, $J = 7.1$ Hz, 3H); ¹³C NMR (CDCl₃) δ 160.3, 138.8, 134.1, 129.1, 62.5, 48.9, 14.9, 14.0; HRMS (ESI) m/z : [M+Na]⁺ calcd for C₈H₁₁N₃O₄Na: 236.0642, found: 236.0643.

Compound **3B**: ¹H NMR (CDCl₃) δ 8.03 (s, 1H), 4.50 (q, $J = 7.2$ Hz, 2H), 4.31 (q, $J = 7.3$ Hz, 2H), 1.50 (t, $J = 7.3$ Hz, 3H), 1.42 (t, $J = 7.2$ Hz, 3H); ¹³C NMR (CDCl₃) δ 158.6, 135.2, 134.4, 131.2, 63.4, 47.7, 15.3, 13.8; HRMS (ESI) m/z : [M+Na]⁺ calcd for C₈H₁₁N₃O₄Na: 236.0642, found: 236.0639.

4.1.2. Ethyl 4-amino-1-ethyl-1H-pyrazole-3-carboxylate (**4A**) and Ethyl 4-amino-1-ethyl-1H-pyrazole-5-carboxylate (**4B**)

After purging with N₂ gas, to a solution of compound **3A** (140 mg, 0.657 mmol) in MeOH (1.3 ml) was added 10% Pd/C

Table 1
Effects of CLB-016 derivatives (in regions 1, 2 and 3) on HIF-1 transcriptional activity and HT1080 cell proliferation

Compd	R ¹	Ar	HRE Luc IC ₅₀ ^a (μM)	HT1080 IC ₅₀ ^a (μM)	AlogP ^b
1 (CLB-016)			19.1 ± 2.8	15.1 ± 1.8	1.18
11Ab			>100	>100	1.74
11Ac			72.0 ± 7.3	50.2 ± 2.9	1.71
11Aaa			19.4 ± 6.2	18.1 ± 0.8	1.38
11Aab			>100	75.0 ± 10.9	1.59
18			71.6 ± 1.1	66.6 ± 2.9	0.62
11Ba			>100	>100	1.04
23			>100	>100	0.72
YC-1			48.4 ± 2.3	30.9 ± 4.3	4.08

^a Data represent the mean ± standard error (n = 3).

^b AlogP was calculated using Pipeline pilot (Accelrys, Inc.).

(6.99 mg, 6.57 μmol). The reaction mixture was purged with H₂ gas and stirred at rt for 22 h. The mixture was filtrated through celite and concentrated. The residue was subjected to column chromatography using amino-functionalized silica gel (EtOAc/MeOH) to furnish the carboxylate **4A** (92.0 mg, 76.8%) as a colorless oil. The isomer **4B** was synthesized in a similar way (66.0 mg, 90.7%).

Compound **4A**: ¹H NMR (CDCl₃) δ 6.99 (1H, s), 4.41 (2H, q, J = 7.2 Hz), 4.13 (2H, q, J = 7.3 Hz), 4.07 (2H, br s), 1.46 (3H, t, J = 7.2 Hz), 1.41 (3H, t, J = 7.2 Hz); ¹³C NMR (CDCl₃) δ 163.7, 135.0, 129.6, 115.8, 60.4, 48.1, 15.4, 14.5; HRMS (ESI) m/z: [M+Na]⁺ calcd for C₈H₁₃N₃O₂Na: 206.0900, found: 206.0904.

Compound **4B**: a colorless oil; ¹H NMR (CDCl₃) δ 7.09 (1H, s), 4.45 (2H, q, J = 7.2 Hz), 4.39 (2H, q, J = 7.2 Hz), 4.10 (2H, br s), 1.41 (3H, t, J = 7.2 Hz), 1.36 (3H, t, J = 7.2 Hz); ¹³C NMR (CDCl₃) δ 160.4, 137.2, 126.9, 116.3, 60.4, 47.5, 15.7, 14.4; HRMS (ESI) m/z: [M+H]⁺ calcd for C₈H₁₄N₃O₂: 184.1081, found: 184.1083.

4.1.3. Synthesis of pyrazoles 7a–e

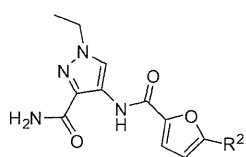
4.1.3.1. Ethyl 5-((3,5-dimethyl-1H-pyrazol-1-yl)methyl)furan-2-carboxylate (**7a**).

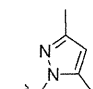
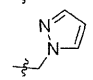
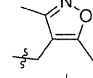
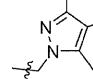
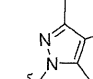
Ethyl 5-(chloromethyl)furan-2-carboxylate (**5a**, 2.0 g, 10.60 mmol) was added to a solution of 3,5-dimethyl-1H-pyrazole (**6a**) (1.019 g, 10.60 mmol), KOtBu (1.547 g, 13.79 mmol) and TBAI (0.392 g, 1.060 mmol) in THF (53 ml) at 0 °C. The mixture was allowed to warm up to rt and was stirred at rt for 24 h. To the reaction mixture was added satd NH₄Cl aq, and then the mixture was extracted with EtOAc. The organic layers were combined, washed with H₂O and brine, dried over Na₂SO₄, and concentrated in vacuo. The residue was subjected to silica gel column chromatography (hexane/EtOAc), which yielded the pyrazole **7a** (1.25 g, 47.5%) as a brown oil. Pyrazoles **7b–e** were synthesized in a similar way.

Compound **7a**: yield, 47.5%; a brown oil; ¹H NMR (CDCl₃) δ 7.07 (d, J = 3.4 Hz, 1H), 6.18 (d, J = 3.7 Hz, 1H), 5.84 (s, 1H), 5.21 (s, 2H),

Table 2

Effects of CLB-016 derivatives (in region 4) on HIF-1 transcriptional activity and HT1080 cell proliferation



Compd	R ²	HRE Luc IC ₅₀ ^a (μM)	HT1080 IC ₅₀ ^a (μM)	ALogP ^b
1 (CLB-016)		19.1 ± 2.8	15.1 ± 1.8	1.18
24		81.8 ± 6.9	75.1 ± 0.2	0.75
25		>100	>100	1.17
11Ad		8.7 ± 0.6	7.4 ± 0.2	1.84
11Ae		8.1 ± 0.2	7.0 ± 0.3	1.93
YC-1		48.4 ± 2.3	30.9 ± 4.3	4.08

^a Data represent the mean ± standard error ($n = 3$).^b ALogP was calculated using Pipeline pilot (Accelrys, Inc.).

4.34 (q, $J = 7.2$ Hz, 2H), 2.28 (s, 3H), 2.21 (s, 3H), 1.36 (t, $J = 7.1$ Hz, 3H); ¹³C NMR (CDCl₃) δ 158.6, 154.7, 148.3, 144.4, 139.5, 118.7, 109.7, 105.8, 60.9, 46.0, 14.3, 13.5, 11.0; HRMS (ESI) m/z : [M+Na]⁺ calcd for C₁₃H₁₆N₂O₃Na: 271.1053, found: 271.1046.

4.1.3.2. Methyl 5-((3,5-dimethyl-1H-pyrazol-1-yl)methyl)thiophene-2-carboxylate (7b). Yield, 42.7%; a white solid; ¹H NMR (CDCl₃) δ 7.63 (d, $J = 3.9$ Hz, 1H), 6.86–6.84 (m, 1H), 5.84 (s, 1H), 5.33 (s, 2H), 3.84 (s, 3H), 2.23 (s, 3H), 2.23 (s, 3H); ¹³C NMR (CDCl₃) δ 162.4, 148.3, 147.4, 138.9, 133.5, 133.0, 125.8, 106.0, 52.1, 47.8, 13.5, 11.0; HRMS (ESI) m/z : [M+H]⁺ calcd for C₁₂H₁₅N₂O₂S: 251.0849, found: 251.0845.

4.1.3.3. Methyl 3-((3,5-dimethyl-1H-pyrazol-1-yl)methyl)benzoate (7c). After extraction, washing and drying, evaporation of the solvent gave a residue that was used without further purification in the next step.

4.1.3.4. Ethyl 5-((4-chloro-3,5-dimethyl-1H-pyrazol-1-yl)methyl)furan-2-carboxylate (7d). Yield, 55.4%, a pale yellow solid; ¹H NMR (CDCl₃) δ 7.08 (d, $J = 3.4$ Hz, 1H), 6.25–6.22 (m, 1H), 5.21 (s, 2H), 4.34 (q, $J = 7.1$ Hz, 2H), 2.28 (s, 3H), 2.20 (s, 3H), 1.36 (t, $J = 7.1$ Hz, 3H); ¹³C NMR (CDCl₃) δ 158.6, 153.7, 145.4, 144.7, 136.1, 118.6, 110.2, 61.1, 46.8, 29.7, 14.3, 11.2, 9.4; HRMS (ESI) m/z : [M+Na]⁺ calcd for C₁₃H₁₅ClN₂O₃Na: 305.0663, found: 305.0666.

4.1.3.5. Ethyl 5-((4-bromo-3,5-dimethyl-1H-pyrazol-1-yl)methyl)furan-2-carboxylate (7e). Yield, 41.5%, a pale yellow powder; ¹H NMR (CDCl₃) δ 7.08 (d, $J = 3.4$ Hz, 1H), 6.24 (d, $J = 3.7$ Hz, 1H), 5.24 (s, 2H), 4.34 (q, $J = 7.1$ Hz, 2H), 2.30 (s, 3H), 2.20 (s, 3H), 1.36 (t, $J = 7.1$ Hz, 3H); ¹³C NMR (CDCl₃) δ 158.5, 153.8, 146.9, 144.7, 137.7, 118.6, 110.2, 95.0, 61.1, 47.0, 14.3, 12.3, 10.4; HRMS (ESI) m/z : [M+Na]⁺ calcd for C₁₃H₁₅BrN₂O₃Na: 349.0158, found: 349.0149.

4.1.4. Synthesis of carboxylic acids 8a–e

4.1.4.1. 5-((3,5-Dimethyl-1H-pyrazol-1-yl)methyl)furan-2-carboxylic acid (8a). A solution of 5 N NaOH (7.25 ml, 36.2 mmol) was added to a solution of compound **7a** (3.0 g, 12.08 mmol) in EtOH (60.4 ml), which was stirred at rt for 24 h. The aqueous phase was acidified to a pH of approx. 3 with 6 N HCl on ice. The majority of the solvent was removed on a rotary evaporator. After the precipitate was filtrated and washed with H₂O, the carboxylic acid **8a** was obtained as a pale yellow powder (1.5 g, 6.81 mmol, 56.4%). Carboxylic acids **8b–e** were synthesized in a similar way.

Compound 8a: yield, 56.4%; a pale yellow powder; ¹H NMR (DMSO-*d*₆) δ 13.07 (s, 1H), 7.14 (d, $J = 3.5$ Hz, 1H), 6.46 (d, $J = 2.9$ Hz, 1H), 5.84 (s, 1H), 5.25 (s, 2H), 2.26 (s, 3H), 2.07 (s, 3H); ¹³C NMR (DMSO-*d*₆) δ 159.1, 154.7, 146.3, 144.4, 139.0, 118.5, 110.3, 105.2, 45.0, 13.2, 10.5; HRMS (ESI) m/z : [M–H][–] calcd for C₁₁H₁₁N₂O₃: 219.0775, found: 219.0769.

4.1.4.2. 5-((3,5-Dimethyl-1H-pyrazol-1-yl)methyl)thiophene-2-carboxylic acid (8b). Yield, 46.4%; a pale yellow powder; ¹H NMR (DMSO-*d*₆) δ 13.0 (s, 1H), 7.56 (d, $J = 3.6$ Hz, 1H), 7.01 (d, $J = 3.6$ Hz, 1H), 5.84 (s, 1H), 5.38 (s, 2H), 2.21 (s, 3H), 2.09 (s, 3H); ¹³C NMR (DMSO-*d*₆) δ 162.7, 147.6, 146.6, 138.7, 133.9, 132.9, 126.6, 105.3, 46.8, 13.3, 10.5; HRMS (ESI) m/z : [M–H][–] calcd for C₁₁H₁₁N₂O₂S: 235.0546, found: 235.0539.

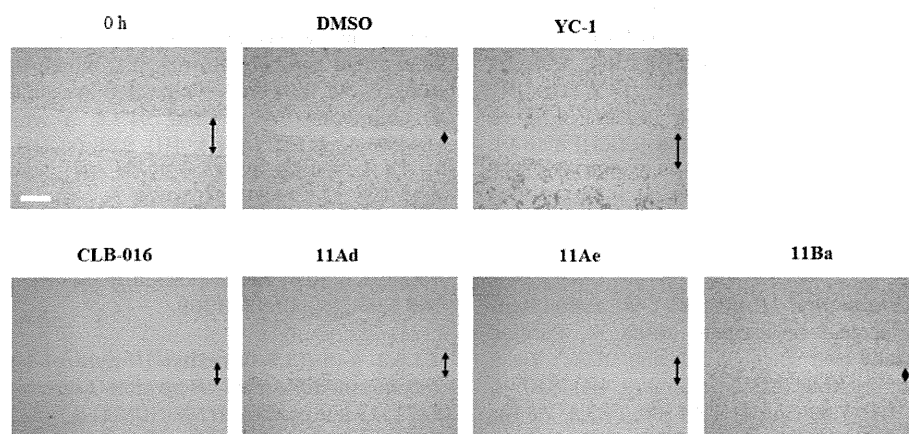


Figure 3. Inhibition of HT1080 cell motility by CLB-016 (**1**) and its derivatives. Each compound (100 μM) was added to scratched monolayers. Representative images of HT1080 cell migration after 48 h of incubation are shown (Scale bar, 500 μm). Double-headed arrows indicate the scratched wound gaps.

4.1.4.3. 3-((3,5-Dimethyl-1H-pyrazol-1-yl)methyl)benzoic acid (8c). Yield, 73.0% (from 2 steps); a white powder; $^1\text{H NMR}$ (DMSO- d_6) δ 13.00 (s, 1H), 7.84 (d, J = 7.5 Hz, 1H), 7.68 (s, 1H), 7.46 (dd, J = 8.1, 7.5 Hz, 1H), 7.33 (d, J = 8.1 Hz, 1H), 5.87 (s, 1H), 5.26 (s, 2H), 2.15 (s, 3H), 2.10 (s, 3H); $^{13}\text{C NMR}$ (DMSO- d_6) δ 167.1, 146.2, 138.8, 138.5, 131.3, 131.0, 128.8, 128.2, 127.6, 105.1, 51.1, 13.3, 10.6; HRMS (ESI) m/z : $[\text{M}-\text{H}]^-$ calcd for $\text{C}_{13}\text{H}_{13}\text{N}_2\text{O}_2$: 229.0982, found: 229.0974.

4.1.4.4. 5-((4-Chloro-3,5-dimethyl-1H-pyrazol-1-yl)methyl)furan-2-carboxylic acid (8d). Yield, 79.8%; a white powder; $^1\text{H NMR}$ (DMSO- d_6) δ 13.09 (s, 1H), 7.15 (d, J = 3.4 Hz, 1H), 6.54 (d, J = 3.4 Hz, 1H), 5.33 (s, 2H), 2.26 (s, 3H), 2.08 (s, 3H); $^{13}\text{C NMR}$ (DMSO- d_6) δ 159.1, 153.8, 144.7, 143.5, 135.7, 118.5, 110.8, 106.5, 46.1, 11.0, 9.0; HRMS (ESI) m/z : $[\text{M}-\text{H}]^-$ calcd for $\text{C}_{11}\text{H}_{10}\text{ClN}_2\text{O}_3$: 253.0385, found: 253.0378.

4.1.4.5. 5-((4-Bromo-3,5-dimethyl-1H-pyrazol-1-yl)methyl)furan-2-carboxylic acid (8e). Yield, 92.7%; a white powder; $^1\text{H NMR}$ (DMSO- d_6) δ 13.12 (s, 1H), 7.15 (d, J = 3.4 Hz, 1H), 6.54 (d, J = 3.4 Hz, 1H), 5.35 (s, 2H), 2.28 (s, 3H), 2.08 (s, 3H); $^{13}\text{C NMR}$ (DMSO- d_6) δ 159.1, 153.8, 145.0, 144.7, 137.4, 118.5, 110.8, 93.4, 46.2, 11.9, 9.9; HRMS (ESI) m/z : $[\text{M}-\text{H}]^-$ calcd for $\text{C}_{11}\text{H}_{10}\text{BrN}_2\text{O}_3$: 296.9880, found: 296.9880.

4.1.5. Synthesis of carboxylates 9Aa–e and 9Ba

4.1.5.1. Ethyl 4-(5-((3,5-dimethyl-1H-pyrazol-1-yl)methyl)furan-2-carboxamido)-1-ethyl-1H-pyrazole-3-carboxylate (9Aa). To a solution of compound **4A** (150 mg, 0.819 mmol) and compound **8a** (180 mg, 0.819 mmol) in DMF (1637 μl) were added HATU (374 mg, 0.982 mmol) and Hunig's base (214 μl , 1.228 mmol). The mixture was stirred at 50 $^\circ\text{C}$ for 5 min in a microwave instrument. The reaction mixture was diluted with H_2O and stirred for 0.5 h. The precipitate was filtrated to give the carboxylic acid **9Aa** (221 mg, 0.57 mmol, 70.0%) as a white powder. Carboxylates **9Ab–e** and **9Ba** were synthesized in a similar way.

Compound **9Aa**: yield, 70.0%; a white cotton; $^1\text{H NMR}$ (CDCl_3) δ 9.90 (1H, s), 8.29 (1H, s), 7.13 (d, J = 3.4 Hz, 1H), 6.31 (d, J = 3.4 Hz, 1H), 5.86 (s, 1H), 5.25 (s, 2H), 4.49 (q, J = 7.1 Hz, 2H), 4.25 (q, J = 7.3 Hz, 2H), 2.39 (s, 3H), 2.22 (s, 3H), 1.53 (t, J = 7.3 Hz, 3H), 1.47 (t, J = 7.1 Hz, 3H); $^{13}\text{C NMR}$ (CDCl_3) δ 163.8, 155.1, 153.2, 148.4, 147.0, 139.6, 130.1, 124.7, 121.1, 116.2, 110.5, 105.9, 61.3, 48.5, 45.8, 15.4, 14.5, 13.5, 11.1; HRMS (ESI) m/z : $[\text{M}+\text{Na}]^+$ calcd for $\text{C}_{19}\text{H}_{23}\text{N}_5\text{O}_4\text{Na}$: 408.1642, found: 408.1646.

4.1.5.2. Ethyl 4-(5-((3,5-dimethyl-1H-pyrazol-1-yl)methyl)thiophene-2-carboxamido)-1-ethyl-1H-pyrazole-3-carboxylate (9Ab). Purified by column chromatography over silica gel (hexane/EtOAc). Yield, 74.7%; a white powder; $^1\text{H NMR}$ (CDCl_3) δ 9.74 (s, 1H), 8.27 (s, 1H), 7.49 (d, J = 4.1 Hz, 1H), 6.88 (d, J = 4.1 Hz, 1H), 5.85 (s, 1H), 5.35 (s, 2H), 4.47 (q, J = 7.2 Hz, 2H), 4.24 (q, J = 7.3 Hz, 2H), 2.25 (s, 3H), 2.24 (s, 3H), 1.52 (t, J = 7.2 Hz, 3H), 1.45 (t, J = 7.0 Hz, 3H); $^{13}\text{C NMR}$ (CDCl_3) δ 164.1, 158.6, 148.4, 146.1, 139.0, 137.9, 129.8, 128.6, 126.2, 125.2, 121.0, 106.1, 61.4, 48.5, 47.8, 15.4, 14.5, 13.5, 11.1. HRMS (ESI) m/z : $[\text{M}+\text{Na}]^+$ calcd for $\text{C}_{19}\text{H}_{23}\text{N}_5\text{O}_3\text{SNa}$: 424.1414, found: 424.1416.

4.1.5.3. Ethyl 4-(3-((3,5-dimethyl-1H-pyrazol-1-yl)methyl)benzamido)-1-ethyl-1H-pyrazole-3-carboxylate (9Ac). Purified by column chromatography over silica gel (hexane/EtOAc). Yield, 93.0%; a pale yellow oil; $^1\text{H NMR}$ (CDCl_3) δ 9.98 (s, 1H), 8.37 (s, 1H), 7.81 (d, J = 7.8 Hz, 1H), 7.69 (s, 1H), 7.44 (dd, J = 7.8, 7.8 Hz, 1H), 7.22 (d, J = 7.6 Hz, 1H), 5.88 (s, 1H), 5.30 (s, 2H), 4.49 (q, J = 7.1 Hz, 2H), 4.26 (q, J = 7.3 Hz, 2H), 2.26 (s, 3H), 2.18 (s, 3H), 1.54 (t, J = 7.3 Hz, 3H), 1.47 (t, J = 7.1 Hz, 3H); $^{13}\text{C NMR}$ (CDCl_3) δ

164.2, 163.8, 148.0, 139.2, 138.5, 133.8, 130.2, 130.0, 129.3, 126.0, 125.6, 125.5, 121.1, 105.8, 61.4, 52.2, 48.5, 15.4, 14.4, 13.5, 11.1. HRMS (ESI) m/z : $[\text{M}+\text{Na}]^+$ calcd for $\text{C}_{21}\text{H}_{25}\text{N}_5\text{O}_3\text{Na}$: 418.1849, found: 418.1841.

4.1.5.4. Ethyl 4-(5-((4-chloro-3,5-dimethyl-1H-pyrazol-1-yl)methyl)furan-2-carboxamido)-1-ethyl-1H-pyrazole-3-carboxylate (9Ad). Yield, 71.1%; a white powder; $^1\text{H NMR}$ (CDCl_3) δ 9.94 (s, 1H), 8.28 (s, 1H), 7.13 (d, J = 3.7 Hz, 1H), 6.37 (d, J = 3.4 Hz, 1H), 5.25 (s, 2H), 4.50 (q, J = 7.2 Hz, 2H), 4.25 (q, J = 7.4 Hz, 2H), 2.40 (s, 3H), 2.21 (s, 3H), 1.53 (t, J = 7.3 Hz, 3H), 1.47 (t, J = 7.2 Hz, 3H); $^{13}\text{C NMR}$ (CDCl_3) δ 163.9, 154.9, 152.3, 147.2, 145.5, 136.0, 130.1, 124.7, 121.0, 116.1, 110.9, 108.5, 61.4, 48.5, 46.7, 15.4, 14.5, 11.4, 9.5; HRMS (ESI) m/z : $[\text{M}+\text{Na}]^+$ calcd for $\text{C}_{19}\text{H}_{22}\text{N}_5\text{O}_4\text{ClNa}$: 442.1252, found: 442.1266.

4.1.5.5. Ethyl 4-(5-((4-bromo-3,5-dimethyl-1H-pyrazol-1-yl)methyl)furan-2-carboxamido)-1-ethyl-1H-pyrazole-3-carboxylate (9Ae). Yield, 67.9%; a white powder; $^1\text{H NMR}$ (CDCl_3) δ 9.94 (1H, s), 8.28 (1H, s), 7.13 (1H, d, J = 3.4 Hz), 6.37 (1H, d, J = 3.4 Hz), 5.27 (2H, s), 4.50 (2H, q, J = 7.1 Hz), 4.25 (2H, q, J = 7.3 Hz), 2.42 (3H, s), 2.22 (3H, s), 1.53 (3H, t, J = 7.3 Hz), 1.47 (3H, t, J = 7.2 Hz); $^{13}\text{C NMR}$ (CDCl_3) δ 163.9, 154.9, 152.2, 147.2, 147.0, 137.8, 130.1, 124.7, 121.0, 116.1, 110.9, 94.9, 61.4, 48.5, 46.8, 15.4, 14.5, 12.3, 10.4; HRMS (ESI) m/z : $[\text{M}+\text{Na}]^+$ calcd for $\text{C}_{19}\text{H}_{22}\text{N}_5\text{O}_4\text{BrNa}$: 486.0747, found: 486.0742.

4.1.5.6. Ethyl 4-(5-((3,5-dimethyl-1H-pyrazol-1-yl)methyl)furan-2-carboxamido)-1-ethyl-1H-pyrazole-5-carboxylate (9Ba). Purified by column chromatography over silica gel (hexane/EtOAc). Yield, 42.5%; a white powder; $^1\text{H NMR}$ (CDCl_3) δ 9.67 (s, 1H), 8.37 (s, 1H), 7.14 (d, J = 3.6 Hz, 1H), 6.28 (d, J = 3.2 Hz, 1H), 5.85 (s, 1H), 5.23 (s, 2H), 4.54 (q, J = 6.8 Hz, 2H), 4.50 (q, J = 7.2 Hz, 2H), 2.33 (s, 3H), 2.22 (s, 3H), 1.50 (t, J = 7.2 Hz, 3H), 1.43 (t, J = 7.2 Hz, 3H); $^{13}\text{C NMR}$ (CDCl_3) δ 159.9, 155.1, 152.9, 148.3, 147.2, 139.4, 130.3, 127.6, 118.4, 116.3, 110.7, 106.0, 61.5, 48.1, 45.9, 15.8, 14.4, 13.5, 11.1; HRMS (ESI) m/z : $[\text{M}+\text{Na}]^+$ calcd for $\text{C}_{19}\text{H}_{23}\text{N}_5\text{O}_4\text{Na}$: 408.1642, found: 408.1649.

4.1.6. Synthesis of carboxylic acids 10Aa–e and 10Ba

4.1.6.1. 4-(5-((3,5-Dimethyl-1H-pyrazol-1-yl)methyl)furan-2-carboxamido)-1-ethyl-1H-pyrazole-3-carboxylic acid (10Aa). 5 N NaOH aq (311 μl , 1.557 mmol) was added to a solution of compound **9Aa** (200 mg, 0.519 mmol) in EtOH (5 ml), and then the mixture was stirred at rt for 9 h. The reaction mixture was adjusted to a pH of approx. 3 with 5 N HCl aq on ice. The majority of the solvent was removed on a rotary evaporator. After the precipitate was filtrated and washed with H_2O , the carboxylic acid **10Aa** was obtained as a white powder (169 mg, 0.47 mmol, 91.1%). Carboxylic acids **10Ab–e** and **10Ba** were synthesized in a similar way.

Compound **10Aa**: yield, 91.1%; a white powder; $^1\text{H NMR}$ (DMSO- d_6) δ 13.37 (br s, 1H), 9.86 (s, 1H), 8.35 (s, 1H), 7.19 (d, J = 3.4 Hz, 1H), 6.58 (d, J = 3.7 Hz, 1H), 5.84 (s, 1H), 5.28 (s, 2H), 4.22 (q, J = 7.2 Hz, 2H), 2.39 (s, 3H), 2.06 (s, 3H), 1.39 (t, J = 7.3 Hz, 3H); $^{13}\text{C NMR}$ (DMSO- d_6) δ 165.0, 153.8, 153.8, 146.5, 146.3, 139.2, 130.2, 123.3, 121.3, 116.1, 111.1, 105.1, 47.4, 44.7, 15.2, 13.3, 10.6; HRMS (ESI) m/z : $[\text{M}-\text{H}]^-$ calcd for $\text{C}_{17}\text{H}_{18}\text{N}_5\text{O}_4$: 356.1364, found: 356.1369.

4.1.6.2. 4-(5-((3,5-Dimethyl-1H-pyrazol-1-yl)methyl)thiophene-2-carboxamido)-1-ethyl-1H-pyrazole-3-carboxylic acid (10Ab). Yield, 93.7%; a white powder; $^1\text{H NMR}$ (DMSO- d_6) δ 13.30 (br s, 1H), 9.84 (s, 1H), 8.26 (s, 1H), 7.55 (d, J = 4.1 Hz, 1H), 7.07 (d, J = 4.1 Hz, 1H), 5.84 (s, 1H), 5.40 (s, 2H), 4.20 (q, J = 7.3 Hz, 2H), 2.21 (s, 3H), 2.09 (s, 3H), 1.37 (t, J = 7.2 Hz, 3H); $^{13}\text{C NMR}$ (DMSO- d_6) δ 164.7, 157.6, 146.5, 146.3, 138.6, 137.4, 130.9,

128.5, 126.8, 123.4, 121.7, 105.2, 47.3, 46.7, 15.2, 13.2, 10.5; HRMS (ESI) m/z : $[M-H]^-$ calcd for $C_{17}H_{18}N_5O_3S$: 372.1136, found: 372.1132.

4.1.6.3. 4-(3-((3,5-Dimethyl-1H-pyrazol-1-yl)methyl)benzamido)-1-ethyl-1H-pyrazole-3-carboxylic acid (10Ac). After the reaction mixture was adjusted to a pH of approx. 3, evaporation of the solvent gave a white powder that was used without further purification to use in the next step.

4.1.6.4. 4-(5-((4-Chloro-3,5-dimethyl-1H-pyrazol-1-yl)methyl)-furan-2-carboxamido)-1-ethyl-1H-pyrazole-3-carboxylic acid (10Ad). Yield, 95.4%; a white powder; 1H NMR (DMSO- d_6) δ 13.37 (br s, 1H), 9.86 (s, 1H), 8.35 (s, 1H), 7.20 (d, $J = 3.4$ Hz, 1H), 6.66 (d, $J = 3.4$ Hz, 1H), 5.37 (s, 2H), 4.23 (q, $J = 7.2$ Hz, 2H), 2.40 (s, 3H), 2.08 (s, 3H), 1.39 (t, $J = 7.3$ Hz, 3H); ^{13}C NMR (DMSO- d_6) δ 165.0, 153.8, 152.9, 146.5, 143.6, 135.9, 130.2, 123.3, 121.4, 116.1, 111.6, 106.5, 47.4, 45.8, 15.2, 11.0, 9.1; HRMS (ESI) m/z : $[M-H]^-$ calcd for $C_{17}H_{17}N_5O_4Cl$: 390.0974, found: 390.0972.

4.1.6.5. 4-(5-((4-Bromo-3,5-dimethyl-1H-pyrazol-1-yl)methyl)-furan-2-carboxamido)-1-ethyl-1H-pyrazole-3-carboxylic acid (10Ae). Yield, 96.8%; a white powder; 1H NMR (DMSO- d_6) δ 13.38 (br s, 1H), 9.87 (s, 1H), 8.35 (s, 1H), 7.20 (d, $J = 3.7$ Hz, 1H), 6.66 (d, $J = 3.7$ Hz, 1H), 5.39 (s, 2H), 4.23 (q, $J = 7.2$ Hz, 2H), 2.41 (s, 3H), 2.08 (s, 3H), 1.39 (t, $J = 7.3$ Hz, 3H); ^{13}C NMR (DMSO- d_6) δ 165.0, 153.8, 152.9, 146.5, 145.2, 137.6, 130.2, 123.3, 121.4, 116.1, 111.6, 93.4, 47.4, 45.9, 15.2, 11.9, 10.0; HRMS (ESI) m/z : $[M-H]^-$ calcd for $C_{17}H_{17}BrN_5O_4$: 434.0469, found: 434.0462.

4.1.6.6. 4-(5-((3,5-Dimethyl-1H-pyrazol-1-yl)methyl)furan-2-carboxamido)-1-ethyl-1H-pyrazole-5-carboxylic acid (10Ba). Yield, 89.7%; a pale yellow powder; 1H NMR (DMSO- d_6) δ 9.75 (s, 1H), 8.12 (s, 1H), 7.20 (d, $J = 3.5$ Hz, 1H), 6.58 (d, $J = 3.5$ Hz, 1H), 5.84 (s, 1H), 5.27 (s, 2H), 4.48 (q, $J = 7.2$ Hz, 2H), 2.36 (s, 3H), 2.06 (s, 3H), 1.33 (t, $J = 7.2$ Hz, 3H); ^{13}C NMR (DMSO- d_6) δ 161.1, 154.2, 153.8, 146.4, 146.2, 139.1, 129.3, 126.2, 119.4, 116.2, 111.0, 105.1, 47.0, 44.6, 15.5, 13.2, 10.6; HRMS (ESI) m/z : $[M-H]^-$ calcd for $C_{17}H_{18}N_5O_4$: 356.1364, found: 356.1359.

4.1.7. Synthesis of carboxamides 1, 11Aa–b, 11Ab–e and 11Ba

To a solution of compound **10Aa** (90 mg, 0.252 mmol) and ammonium chloride (67.4 mg, 1.259 mmol) in DMF (1.5 ml) were added HATU (115 mg, 0.302 mmol) and Hunig's base (286 μ l, 1.637 mmol). The mixture was stirred for 5 min at 50 °C in a microwave instrument. The reaction mixture was diluted with H_2O and stirred for 0.5 h. The precipitate was filtrated, and then purified by column chromatography over amino-functionalized silica gel (hexane/EtOAc) to give the carboxamide **1** (76 mg, 0.21 mmol, 84.7%) as a white powder. Carboxamides **11Aa–b**, **11Ab–e** and **11Ba** were synthesized in a similar way.

Compound **1**: yield, 84.7%; a white powder; mp 209.7–210.2 °C; IR (cm^{-1}) 3522, 3404, 3346, 3009, 1668, 1605, 1583, 1553, 1420, 1375, 1331, 1236, 1221, 1213, 1138, 1016, 964; 1H NMR ($CDCl_3$) δ 10.27 (s, 1H), 8.25 (s, 1H), 7.11 (d, $J = 3.4$ Hz, 1H), 6.74 (br s, 1H), 6.29 (d, $J = 3.7$ Hz, 1H), 5.85 (s, 1H), 5.62 (br s, 1H), 5.24 (s, 2H), 4.16 (q, $J = 7.3$ Hz, 2H), 2.39 (s, 3H), 2.21 (s, 3H), 1.51 (t, $J = 7.3$ Hz, 3H); ^{13}C NMR ($CDCl_3$) δ 165.7, 155.2, 153.2, 148.3, 147.1, 139.7, 131.6, 123.4, 121.4, 116.0, 110.5, 105.8, 48.1, 45.8, 15.3, 13.5, 11.1; HRMS (ESI) m/z : $[M+H]^+$ calcd for $C_{17}H_{21}N_6O_3$: 357.1669, found: 357.1670.

4.1.7.1. 4-(5-((3,5-Dimethyl-1H-pyrazol-1-yl)methyl)furan-2-carboxamido)-1-ethyl-N-methyl-1H-pyrazole-3-carboxamide (11Aaa). The reaction mixture was stirred for 5 h at rt. Yield, 24.5%; a white powder; mp 178.9–179.0 °C; IR (cm^{-1}) 3431, 3335, 3009, 1655, 1584, 1554, 1437, 1373, 1223, 1209, 1173, 1146, 1016, 962; 1H NMR ($CDCl_3$) δ

10.39 (s, 1H), 8.23 (s, 1H), 7.09 (d, $J = 3.4$ Hz, 1H), 6.82–6.75 (m, 1H), 6.21 (d, $J = 3.4$ Hz, 1H), 5.85 (s, 1H), 5.25 (s, 2H), 4.15 (q, $J = 7.3$ Hz, 2H), 3.01 (d, $J = 5.1$ Hz, 3H), 2.37 (s, 3H), 2.22 (s, 3H), 1.50 (t, $J = 7.3$ Hz, 3H); ^{13}C NMR ($CDCl_3$) δ 164.3, 155.2, 153.4, 148.3, 147.1, 139.7, 132.3, 122.9, 121.3, 115.8, 110.2, 105.8, 48.0, 46.0, 25.4, 15.3, 13.5, 11.1; HRMS (ESI) m/z : $[M+H]^+$ calcd for $C_{18}H_{23}N_6O_3$: 371.1826, found: 371.1812.

4.1.7.2. 4-(5-((3,5-Dimethyl-1H-pyrazol-1-yl)methyl)furan-2-carboxamido)-1-ethyl-N,N-dimethyl-1H-pyrazole-3-carboxamide (11Aab). The reaction mixture was stirred for 5 h at rt. Yield, 30.2%; a white powder; mp 185.8–186.3 °C; IR (cm^{-1}) 3319, 3002, 2955, 1661, 1618, 1603, 1576, 1551, 1533, 1425, 1367, 1213, 1191, 1163, 1136, 1084, 1016, 966; 1H NMR ($CDCl_3$) δ 10.84 (s, 1H), 8.27 (s, 1H), 7.08 (d, $J = 3.5$ Hz, 1H), 6.25 (d, $J = 3.5$ Hz, 1H), 5.84 (s, 1H), 5.24 (s, 2H), 4.17 (q, $J = 7.3$ Hz, 2H), 3.59 (s, 3H), 3.14 (s, 3H), 2.39 (s, 3H), 2.21 (s, 3H), 1.51 (t, $J = 7.2$ Hz, 3H); ^{13}C NMR ($CDCl_3$) δ 164.5, 155.1, 153.1, 148.3, 147.4, 139.8, 133.4, 124.9, 120.5, 115.5, 110.2, 105.8, 47.9, 45.9, 39.0, 36.5, 15.2, 13.5, 11.1; HRMS (ESI) m/z : $[M+H]^+$ calcd for $C_{19}H_{25}N_6O_3$: 385.1982, found: 385.1975.

4.1.7.3. 4-(5-((3,5-Dimethyl-1H-pyrazol-1-yl)methyl)thiophene-2-carboxamido)-1-ethyl-1H-pyrazole-3-carboxamide (11Ab). The reaction mixture was stirred for 13 h at rt. Recrystallized from EtOH. Yield, 64.4%; a white cotton; mp 230.0–230.2 °C; IR (cm^{-1}) 3522, 3402, 3346, 3009, 2959, 1666, 1583, 1545, 1487, 1420, 1375, 1223, 1213, 1171, 1132, 1022, 960, 901; 1H NMR ($CDCl_3$) δ 10.18 (s, 1H), 8.21 (s, 1H), 7.48 (d, $J = 3.9$ Hz, 1H), 6.87 (d, $J = 3.7$ Hz, 1H), 6.68 (br s, 1H), 5.84 (s, 1H), 5.34 (s, 3H), 4.16 (q, $J = 7.3$ Hz, 2H), 2.24 (s, 3H), 2.23 (s, 3H), 1.51 (t, $J = 7.3$ Hz, 3H); ^{13}C NMR ($CDCl_3$) δ 165.9, 158.7, 148.3, 145.9, 139.0, 138.1, 131.3, 128.5, 126.1, 124.0, 121.3, 106.0, 48.1, 47.8, 15.3, 13.5, 11.1; HRMS (ESI) m/z : $[M+H]^+$ calcd for $C_{17}H_{21}N_6O_2S$: 373.1441, found: 373.1441.

4.1.7.4. 4-(3-((3,5-Dimethyl-1H-pyrazol-1-yl)methyl)benzamido)-1-ethyl-1H-pyrazole-3-carboxamide (11Ac). Purified by column chromatography over silica gel (hexane/EtOAc). Yield, 19.0% (from 2 steps); a white powder; mp 152.6–153.5 °C; IR (cm^{-1}) 3522, 3402, 3354, 3018, 1666, 1583, 1539, 1420, 1375, 1329, 1219, 1211; 1H NMR ($CDCl_3$) δ 10.41 (s, 1H), 8.31 (d, $J = 1.2$ Hz, 1H), 7.80 (d, $J = 7.5$ Hz, 1H), 7.74 (s, 1H), 7.42 (t, $J = 7.5$ Hz, 1H), 7.17 (d, $J = 7.5$ Hz, 1H), 6.72 (br s, 1H), 5.87 (s, 1H), 5.41 (br s, 1H), 5.29 (s, 2H), 4.18 (q, $J = 7.3$ Hz, 2H), 2.25 (s, 3H), 2.17 (s, 3H), 1.52 (t, $J = 7.5$ Hz, 3H); ^{13}C NMR ($CDCl_3$) δ 165.9, 163.9, 147.9, 139.3, 138.4, 133.9, 131.6, 130.2, 129.3, 126.1, 125.7, 124.3, 121.4, 105.8, 52.3, 48.1, 15.3, 13.5, 11.2; HRMS (ESI) m/z : $[M+Na]^+$ calcd for $C_{19}H_{22}N_6O_2Na$: 389.1696, found: 389.1681.

4.1.7.5. 4-(5-((4-Chloro-3,5-dimethyl-1H-pyrazol-1-yl)methyl)-furan-2-carboxamido)-1-ethyl-1H-pyrazole-3-carboxamide (11Ad). Yield, 71.9%; a white powder; mp 220.1–220.8 °C; IR (cm^{-1}) 3522, 3404, 3344, 2997, 1668, 1605, 1583, 1553, 1477, 1421, 1377, 1331, 1223, 1209, 1140, 1088, 1016, 962; 1H NMR ($CDCl_3$) δ 10.29 (s, 1H), 8.24 (s, 1H), 7.11 (d, $J = 3.7$ Hz, 1H), 6.70 (br s, 1H), 6.33 (d, $J = 3.4$ Hz, 1H), 5.44 (br s, 1H), 5.23 (s, 2H), 4.17 (q, $J = 7.3$ Hz, 2H), 2.40 (s, 3H), 2.20 (s, 3H), 1.51 (t, $J = 7.3$ Hz, 3H); ^{13}C NMR ($CDCl_3$) δ 165.6, 155.0, 152.4, 147.3, 145.4, 136.0, 131.6, 123.4, 121.4, 115.9, 110.9, 108.5, 48.1, 46.8, 15.3, 11.4, 9.5; HRMS (ESI) m/z : $[M+H]^+$ calcd for $C_{17}H_{20}ClN_6O_3$: 391.1280, found: 391.1282.

4.1.7.6. 4-(5-((4-Bromo-3,5-dimethyl-1H-pyrazol-1-yl)methyl)-furan-2-carboxamido)-1-ethyl-1H-pyrazole-3-carboxamide (11Ae). Yield, 81.6%; a white powder; mp 229.8–230.2 °C; IR

(cm^{-1}) 3522, 3404, 3344, 3009, 1668, 1605, 1585, 1553, 1477, 1421, 1377, 1331, 1221, 1209, 1140, 1072, 1016, 964; ^1H NMR (CDCl_3) δ 10.30 (s, 1H), 8.24 (s, 1H), 7.11 (d, $J = 3.4$ Hz, 1H), 6.72 (br s, 1H), 6.34 (d, $J = 3.7$ Hz, 1H), 5.49 (br s, 1H), 5.26 (s, 2H), 4.17 (q, $J = 7.4$ Hz, 2H), 2.41 (s, 3H), 2.21 (s, 3H), 1.51 (t, $J = 7.3$ Hz, 3H); ^{13}C NMR (CDCl_3) δ 165.6, 155.0, 152.3, 147.3, 146.9, 137.8, 131.6, 123.4, 121.4, 115.9, 110.9, 94.9, 48.1, 46.9, 15.3, 12.3, 10.5; HRMS (ESI) m/z : $[\text{M}+\text{H}]^+$ calcd for $\text{C}_{17}\text{H}_{20}\text{BrN}_6\text{O}_3$: 435.0775, found: 435.0783.

4.1.7.7. 4-(5-((3,5-Dimethyl-1H-pyrazol-1-yl)methyl)furan-2-carboxamido)-1-ethyl-1H-pyrazole-5-carboxamide (11Ba). The reaction mixture was stirred at rt for 5 h. Yield, 47.4%; a white powder; mp 189.9–190.5 °C; IR (cm^{-1}) 3468, 3404, 3292, 2999, 1676, 1604, 1585, 1551, 1474, 1379, 1221, 1209, 1148, 1090, 1016, 970; ^1H NMR (CDCl_3) δ 9.09 (s, 1H), 7.83 (d, $J = 1.2$ Hz, 1H), 7.13 (dd, $J = 3.5, 1.2$ Hz, 1H), 6.42 (br s, 2H), 6.33 (d, $J = 3.5$ Hz, 1H), 5.85 (s, 1H), 5.20 (s, 2H), 4.45 (q, $J = 7.3$ Hz, 2H), 2.31 (s, 3H), 2.20 (s, 3H), 1.48 (t, $J = 7.2$ Hz, 3H); ^{13}C NMR (CDCl_3) δ 161.6, 157.2, 152.9, 148.5, 146.9, 139.3, 133.4, 127.4, 121.3, 116.8, 110.7, 106.0, 47.3, 45.6, 15.6, 13.4, 11.1; HRMS (ESI) m/z : $[\text{M}+\text{H}]^+$ calcd for $\text{C}_{17}\text{H}_{21}\text{N}_6\text{O}_3$: 357.1669, found: 357.1665.

4.1.8. Methyl 4-nitro-1H-pyrazole-3-carboxylate (12)

Acetyl chloride (6.34 ml, 89 mmol) was added to the mixture of 4-nitro-1H-pyrazole-3-carboxylic acid (**2**, 7 g, 44.6 mmol) in MeOH (223 ml) at 0 °C. The mixture was stirred at rt for 16 h. After concentrated in vacuo, the residue was azeotroped with MeOH two times. The residue was diluted with MeOH and EtOAc, and the mixture was adjusted to a pH of approx. 9 with satd NaHCO_3 aq. The mixture was extracted with EtOAc. The organic layer was washed with H_2O and brine, dried over Na_2SO_4 , and concentrated to give the compound **12** (5.545 g, 32.4 mmol, 72.7%) as a white powder.

^1H NMR ($\text{DMSO}-d_6$) δ 14.39 (br s, 1H), 8.99 (s, 1H), 3.89 (s, 3H); ^{13}C NMR ($\text{DMSO}-d_6$) δ 161.1, 138.1, 133.2, 130.9, 52.8; HRMS (ESI) m/z : $[\text{M}-\text{H}]^-$ calcd for $\text{C}_5\text{H}_4\text{N}_3\text{O}_4$: 170.0207, found: 170.0200.

4.1.9. Methyl 4-nitro-1-((2-(trimethylsilyl)ethoxy)methyl)-1H-pyrazole-3-carboxylate (13)

To a solution of methyl 4-nitro-1H-pyrazole-3-carboxylate (**12**, 3.0 g, 17.53 mmol) in THF (88 ml) was added NaH (1.052 g, 26.3 mmol) at 0 °C in an Ar atmosphere. After being stirred for 10 min, SEM-Cl (3.73 ml, 21.04 mmol) was added to the reaction at 0 °C and stirred for another 20 min at rt. The reaction was quenched with H_2O and extracted with EtOAc. The organic layer was washed with brine and dried over Na_2SO_4 . After filtration and concentration, the residue was subjected to silica gel column chromatography to give the compound **13** (2.83 g, 9.39 mmol, 53.6%) as a colorless oil and methyl 4-nitro-1-((2-(trimethylsilyl)ethoxy)methyl)-1H-pyrazole-5-carboxylate **13'** (1.60 g, 5.31 mmol, 30.3%) as a colorless oil.

Compound **13**: ^1H NMR (CDCl_3) δ 8.32 (s, 1H), 5.48 (s, 2H), 4.00 (s, 3H), 3.66–3.62 (m, 2H), 0.97–0.93 (m, 2H), 0.00 (s, 9H); ^{13}C NMR (CDCl_3) δ 160.3, 138.4, 135.2, 129.7, 82.1, 68.4, 53.2, 17.8, –1.5; HRMS (ESI) m/z : $[\text{M}+\text{Na}]^+$ calcd for $\text{C}_{11}\text{H}_{19}\text{N}_3\text{O}_5\text{SiNa}$: 324.0986, found: 324.0982.

Compound **13'**: ^1H NMR (CDCl_3) δ 8.06 (1H, s), 5.61 (2H, s), 4.03 (3H, s), 3.59–3.54 (2H, m), 0.92–0.86 (2H, m), –0.02 (9H, s); ^{13}C NMR (CDCl_3) δ 158.6, 135.3, 135.2, 131.4, 80.8, 67.9, 53.9, 17.6, –1.5; HRMS (ESI) m/z : $[\text{M}+\text{Na}]^+$ calcd for $\text{C}_{11}\text{H}_{19}\text{N}_3\text{O}_5\text{SiNa}$: 324.0986, found: 324.0986.

4.1.10. Methyl 4-amino-1-((2-(trimethylsilyl)ethoxy)methyl)-1H-pyrazole-3-carboxylate (14)

After purging with N_2 gas, 10% Pd/C (32 mg, 0.030 mmol) was added to the solution of compound **13** (913 mg, 3.02 mmol) in

EtOH (15 ml). The reaction mixture was purged with H_2 gas and stirred for 1 h at 40 °C. The mixture was filtrated and concentrated. The residue was subjected to column chromatography over amino-functionalized silica gel (EtOAc/MeOH) to give the compound **14** (580.9 mg, 2.14 mmol, 70.9%) as a colorless oil.

^1H NMR (CDCl_3) δ 7.16 (1H, s), 5.37 (2H, s), 4.12 (2H, br s), 3.94 (3H, s), 3.55–3.51 (2H, m), 0.92–0.88 (2H, m), –0.02 (9H, s); ^{13}C NMR (CDCl_3) δ 164.1, 135.6, 130.3, 115.8, 81.6, 67.0, 51.7, 17.9, –1.4; HRMS (ESI) m/z : $[\text{M}+\text{Na}]^+$ calcd for $\text{C}_{11}\text{H}_{21}\text{N}_3\text{O}_3\text{SiNa}$: 294.1244, found: 294.1235.

4.1.11. Methyl 4-(5-((3,5-dimethyl-1H-pyrazol-1-yl)methyl)furan-2-carboxamido)-1-((2-(trimethylsilyl)ethoxy)methyl)-1H-pyrazole-3-carboxylate (15)

To a solution of compound **14** (0.58 g, 2.137 mmol) and compound **8a** (0.471 g, 2.137 mmol) in DMF (10 ml) were added HATU (0.97 g, 2.56 mmol) and Hunig's Base (0.560 ml, 3.21 mmol). The mixture was stirred for 5 min at 50 °C, 3 times in a microwave instrument. The reaction mixture was diluted with H_2O and satd NaHCO_3 aq and then, the mixture was extracted with EtOAc. The organic layer was washed with H_2O and brine, and dried over Na_2SO_4 , and evaporated. The residue was subjected to silica gel column chromatography (hexane/EtOAc) to give the compound **15** (493 mg, 1.04 mmol, 48.7%) as a white powder.

^1H NMR (CDCl_3) δ 9.86 (s, 1H), 8.46 (s, 1H), 7.14 (d, $J = 3.7$ Hz, 1H), 6.33 (d, $J = 3.7$ Hz, 1H), 5.86 (s, 1H), 5.48 (s, 2H), 5.26 (s, 2H), 4.02 (s, 3H), 3.59–3.55 (m, 2H), 2.39 (s, 3H), 2.23 (s, 3H), 0.94–0.90 (m, 2H), –0.03 (s, 9H); ^{13}C NMR (CDCl_3) δ 164.1, 155.1, 153.2, 148.4, 146.9, 139.6, 130.7, 125.2, 121.6, 116.3, 110.6, 105.9, 81.8, 67.3, 52.2, 45.8, 17.8, 13.5, 11.1, –1.5; HRMS (ESI) m/z : $[\text{M}+\text{Na}]^+$ calcd for $\text{C}_{22}\text{H}_{31}\text{N}_5\text{O}_5\text{SiNa}$: 496.1986, found: 496.1989.

4.1.12. 4-(5-((3,5-Dimethyl-1H-pyrazol-1-yl)methyl)furan-2-carboxamido)-1-((2-(trimethylsilyl)ethoxy)methyl)-1H-pyrazole-3-carboxylic acid (16)

An aqueous solution of 5 N NaOH (624 μl , 3.12 mmol) was added to a solution of compound **15** (493 mg, 1.04 mmol) in EtOH (5 ml), and then the mixture was stirred at rt for 2 h. The pH of the reaction mixture was adjusted to approx. 3 with 6 N HCl on ice. The majority of solvent was removed on a rotary evaporator. After the precipitate was filtrated, the solid was washed with H_2O to give the compound **16** (455 mg, 0.990 mmol, 95.2%) as a white powder.

^1H NMR ($\text{DMSO}-d_6$) δ 9.90 (s, 1H), 8.45 (s, 1H), 7.21 (d, $J = 3.4$ Hz, 1H), 6.59 (d, $J = 3.4$ Hz, 1H), 5.84 (s, 1H), 5.49 (s, 2H), 5.28 (s, 2H), 3.57–3.54 (m, 2H), 2.38 (s, 3H), 2.06 (s, 3H), 0.86–0.82 (m, 2H), –0.05 (s, 9H); ^{13}C NMR ($\text{DMSO}-d_6$) δ 171.7, 165.0, 154.0, 153.8, 146.5, 146.2, 139.3, 123.5, 122.2, 116.2, 111.1, 105.1, 80.5, 66.1, 44.7, 17.1, 13.3, 10.7, –1.4; HRMS (ESI) m/z : $[\text{M}-\text{H}]^-$ calcd for $\text{C}_{21}\text{H}_{28}\text{N}_5\text{O}_5\text{Si}$: 458.1865, found: 458.1869.

4.1.13. 4-(5-((3,5-Dimethyl-1H-pyrazol-1-yl)methyl)furan-2-carboxamido)-1-((2-(trimethylsilyl)ethoxy)methyl)-1H-pyrazole-3-carboxamide (17)

To a solution of compound **16** (90 mg, 0.196 mmol) and ammonium chloride (52.4 mg, 0.979 mmol) in DMF (1 ml) were added HATU (89 mg, 0.235 mmol) and Hunig's base (0.222 ml, 1.273 mmol). The mixture was stirred for 5 min at 50 °C in a microwave instrument. The reaction mixture was diluted with H_2O . The precipitate was filtrated and washed with H_2O to give the compound **17** (75 mg, 0.16 mmol, 83.5%) as a white powder.

^1H NMR (CDCl_3) δ 10.27 (s, 1H), 8.41 (s, 1H), 7.12 (d, $J = 3.4$ Hz, 1H), 6.76 (br s, 1H), 6.30 (d, $J = 3.4$ Hz, 1H), 5.85 (s, 1H), 5.47 (br s, 1H), 5.40 (s, 2H), 5.24 (s, 2H), 3.59–3.54 (m, 2H), 2.40 (d, $J = 0.7$ Hz, 3H), 2.21 (s, 3H), 0.95–0.91 (m, 2H), –0.01 (s, 9H); ^{13}C NMR (CDCl_3) δ 165.4, 155.2, 153.3, 148.3, 147.0, 139.7, 132.8, 123.9, 122.2,

116.1, 110.5, 105.8, 81.2, 67.2, 45.8, 17.7, 13.5, 11.1, –1.4; HRMS (ESI) m/z : $[M+H]^+$ calcd for $C_{21}H_{31}N_6O_4Si$: 459.2170, found: 459.2151.

4.1.14. 4-(5-((3,5-Dimethyl-1H-pyrazol-1-yl)methyl)furan-2-carboxamido)-1H-pyrazole-3-carboxamide (18)

To a suspension of compound **17** (40 mg, 0.087 mmol) in EtOH (174 μ l) was added 2 M HCl/EtOH (436 μ l, 0.872 mmol). The mixture was stirred at 80 °C for 1.5 h in a microwave instrument. After the white precipitate was filtrated, the solid was washed with EtOH. The resultant pellet was suspended in satd $NaHCO_3$ aq, and stirred for 0.5 h. After the white precipitate was filtrated, the solid was washed with H_2O . The residue was subjected to column chromatography over amino-functionalized silica gel ($CH_2Cl_2/MeOH$) to give the compound **18** (15 mg, 0.05 mmol, 52.4%) as a white powder.

Mp 234.6–235.1 °C; IR (cm^{-1}) 3676, 3522, 3447, 3404, 3344, 3007, 1670, 1605, 1583, 1555, 1448, 1420, 1375, 1340, 1300, 1236, 1103, 1016, 968, 943, 881; 1H NMR (DMSO- d_6) δ 13.26 (s, 1H), 10.49 (s, 1H), 8.24 (s, 1H), 7.81 (s, 1H), 7.58 (s, 1H), 7.14 (d, $J = 3.4$ Hz, 1H), 6.57 (d, $J = 3.7$ Hz, 1H), 5.84 (s, 1H), 5.28 (s, 2H), 2.41 (s, 3H), 2.06 (s, 3H); ^{13}C NMR (DMSO- d_6) δ 165.7, 153.7, 153.5, 146.5, 146.4, 139.2, 132.6, 121.7, 119.8, 115.6, 110.9, 105.0, 44.6, 13.2, 10.6; HRMS (ESI) m/z : $[M+H]^+$ calcd for $C_{15}H_{17}N_6O_3$: 329.1356, found: 329.1362.

4.1.15. Methyl 1-(((tert-butoxycarbonyl)amino)methyl)-4-nitro-1H-pyrazole-5-carboxylate (20)

To a solution of compound **12** (1.333 g, 7.79 mmol), K_2CO_3 (1.615 g, 11.68 mmol) and TBAI (0.288 g, 0.779 mmol) in DMF (39 ml) was added *tert*-butyl (2-bromoethyl)carbamate (**19**) (1.92 g, 8.57 mmol). The mixture was stirred at rt for 2 h, and then filtrated on Celite. After concentration, the pellet was suspended in EtOAc and H_2O , and extracted with EtOAc. The organic layer was washed with H_2O and brine, dried over Na_2SO_4 , and concentrated in vacuo. The residue was subjected to column chromatography over silica gel (hexane/EtOAc) to yield compound **20** (271 mg, 11.1%, 0.863 mmol) as a white powder and methyl 1-(((tert-butoxycarbonyl)amino)methyl)-4-nitro-1H-pyrazole-3-carboxylate **20'** (28.6%, 701 mg, 2.228 mmol) as a white powder.

Compound **20**: 1H NMR ($CDCl_3$) δ 8.06 (1H, s), 4.85–4.77 (1H, m), 4.40 (2H, t, $J = 5.5$ Hz), 4.02 (3H, s), 3.60 (2H, q, $J = 5.5$ Hz), 1.42 (9H, s); ^{13}C NMR ($CDCl_3$) δ 158.8, 155.7, 135.8, 134.7, 131.8, 80.0, 53.9, 52.0, 40.2, 28.3; HRMS (ESI) m/z : $[M+Na]^+$ calcd for $C_{12}H_{18}N_4O_6Na$: 337.1118, found: 337.1114.

Compound **20'**: 1H NMR ($CDCl_3$) δ 8.18 (1H, s), 4.91–4.81 (1H, m), 4.39–4.30 (2H, m), 3.99 (3H, s), 3.64–3.56 (2H, m), 1.43 (9H, s); ^{13}C NMR ($CDCl_3$) δ 160.5, 155.9, 138.8, 134.2, 131.0, 80.4, 53.2, 53.2, 40.1, 28.3; HRMS (ESI) m/z : $[M+Na]^+$ calcd for $C_{12}H_{18}N_4O_6Na$: 337.1118, found: 337.1113.

4.1.16. 3-Nitro-6,7-dihydropyrazolo[1,5-a]pyrazin-4(5H)-one (21)

2 M HCl/EtOH (3.6 ml, 7.22 mmol) was added to a solution of compound **20** (227 mg, 0.722 mmol) in EtOH (1.5 ml) at rt. The mixture was stirred at 50 °C for 1 h. The precipitate was collected by filtration as a white powder, and subjected to the next reaction. The mixture of the white powder and Et_3N (0.150 ml, 1.077 mmol) in toluene (5 ml) was stirred at 100 °C for 1 h. After cooling to room temperature, H_2O was added to the reaction mixture. The precipitate was filtered, and dried in vacuo to give the compound **21** (60 mg, 0.329 mmol, 45.6%) as a white powder.

1H NMR (DMSO- d_6) δ 8.71 (1H, br s), 8.35 (1H, s), 4.41–4.38 (2H, m), 3.67–3.61 (2H, m); ^{13}C NMR (DMSO- d_6) δ 154.6, 136.3, 134.0, 129.4, 47.3, 38.4; HRMS (ESI) m/z : $[M+Na]^+$ calcd for $C_6H_6N_4O_3Na$: 205.0332, found: 205.0333.

4.1.17. 3-Amino-6,7-dihydropyrazolo[1,5-a]pyrazin-4(5H)-one (22)

After being purged with N_2 gas, 10% (w/w) Pd/C (3.80 mg, 3.57 μ mol) was added to a solution of compound **21** (65 mg, 0.357 mmol) in EtOH (2 ml). The reaction mixture was purged with H_2 gas and stirred at 40 °C for 1.5 h. The mixture was filtrated and concentrated. The residue was subjected to column chromatography over amino-functionalized silica gel (EtOAc/MeOH) to give the compound **22** (46 mg, 0.298 mmol, 83.5%) as a white powder.

1H NMR (DMSO- d_6) δ 7.75 (1H, s), 6.99 (1H, s), 4.67 (2H, s), 4.10–4.05 (2H, m), 3.54–3.48 (2H, m); ^{13}C NMR (DMSO- d_6) δ 160.9, 134.9, 126.9, 117.1, 45.8, 39.4; HRMS (ESI) m/z : $[M+Na]^+$ calcd for $C_6H_8N_4ONa$: 175.0596, found: 175.0589.

4.1.18. 5-((3,5-Dimethyl-1H-pyrazol-1-yl)methyl)-N-(4-oxo-4,5,6,7-tetrahydropyrazolo[1,5-a]pyrazin-3-yl)furan-2-carboxamide (23)

HATU (135 mg, 0.355 mmol) and Hunig's base (77 μ l, 0.444 mmol) were added to a solution of compound **22** (45 mg, 0.296 mmol) and compound **8a** (65.1 mg, 0.296 mmol) in DMF (1.5 ml) at rt. The mixture was stirred at 50 °C for 5 min in a microwave instrument. The mixture was diluted in H_2O and satd $NaHCO_3$ aq, and extracted with EtOAc. The organic layer was washed with H_2O and brine, and dried over Na_2SO_4 , and concentrated in vacuo. The residue was subjected to a column chromatography over silica gel (hexane/EtOAc) to give the compound **23** (44 mg, 0.123 mmol, 41.6%) as a yellow powder.

Mp 288.4–289.6 °C; IR (cm^{-1}) 3418, 3254, 2997, 1668, 1610, 1551, 1491, 1429, 1379, 1354, 1335, 1304, 1223, 1209, 1142, 1055, 1016, 970; 1H NMR (DMSO- d_6) δ 9.56 (s, 1H), 8.46 (s, 1H), 8.04 (s, 1H), 7.20 (d, $J = 3.7$ Hz, 1H), 6.58 (d, $J = 3.7$ Hz, 1H), 5.83 (s, 1H), 5.28 (s, 2H), 4.32–4.25 (m, 2H), 3.68–3.61 (m, 2H), 2.39 (s, 3H), 2.06 (s, 3H); ^{13}C NMR (DMSO- d_6) δ 160.0, 154.1, 153.8, 146.4, 146.1, 139.2, 129.4, 123.0, 120.4, 116.2, 111.0, 105.0, 45.6, 44.6, 13.2, 10.5; HRMS (ESI) m/z : $[M+H]^+$ calcd for $C_{17}H_{19}N_6O_3$: 355.1513, found: 355.1501.

4.1.19. 4-(5-(((1H-Pyrazol-1-yl)methyl)furan-2-carboxamido)-1-ethyl-1H-pyrazole-3-carboxamide (24)

Compound **24** was prepared according to the synthetic procedure in a similar way of CLB-016 (**1**) starting from a commercially available 5-((1H-pyrazol-1-yl)methyl)furan-2-carboxylic acid.

Yield: 32.8% in 3 steps as a white powder; mp 199.5–200.3 °C; IR (cm^{-1}) 3522, 3402, 3344, 3009, 1668, 1607, 1585, 1555, 1420, 1375, 1330, 1217, 1209, 1135, 1088, 1016, 962; 1H NMR ($CDCl_3$) δ 10.33 (s, 1H), 8.24 (s, 1H), 7.60 (d, $J = 2.4$ Hz, 1H), 7.55 (d, $J = 1.7$ Hz, 1H), 7.12 (d, $J = 3.4$ Hz, 1H), 6.74 (br s, 1H), 6.40 (d, $J = 3.4$ Hz, 1H), 6.32 (dd, $J = 2.1, 2.1$ Hz, 1H), 5.58 (s, 1H), 5.40 (s, 2H), 4.17 (q, $J = 7.3$ Hz, 2H), 1.51 (t, $J = 7.3$ Hz, 3H); ^{13}C NMR ($CDCl_3$) δ 165.7, 155.1, 152.2, 147.4, 140.0, 131.6, 129.6, 123.4, 121.4, 115.8, 111.1, 106.5, 48.7, 48.1, 15.3; HRMS (ESI) m/z : $[M+H]^+$ calcd for $C_{15}H_{17}N_6O_3$: 329.1356, found: 329.1348.

4.2. Biology

4.2.1. Cell-based HRE-driven luciferase reporter assay

x5HRE/HT1080 cells, stable transformant cell lines with a 5xHRE/pGL3/VEGF/E1b reporter plasmid,¹² were cultured in Dulbecco's modified Eagle's medium containing 10% fetal bovine serum at 37 °C in a humidified 5% CO_2 incubator. For reporter assay, cells (1.0×10^4) were seeded in 96-well plates (in 100 μ l) and pre-incubated for 24 h. After 1 h from the addition of chemical compounds, the cells were incubated under hypoxia (1% O_2) for 24 h. The cells were washed with ice-cold phosphate-buffered saline (PBS) 3 times, followed by lysis in 30 μ l of lysis buffer (20 mM Tris/HCl pH 7.5, 150 mM NaCl, 1 mM EDTA and 0.1% Triton X-100).

Twenty-microliter of the cellular lysate was employed for the luciferin-luciferase assay (50 mM Tris pH 8.0, 5 mM MgSO₄, 0.125 mM D-luciferin, 0.5 mM ATP, and 0.5 mM CoA). Epiluminescence was measured using an EnVision luminometer (Perkin Elmer). Each compound was tested in triplicate. To calculate the relative luciferase activity, the luminescence units were normalized with total protein content in each well.

4.2.2. Cell proliferation assay

HT1080 cells (1.0×10^3 cells/well) were seeded in a 96-well plate (in 100 μ l) and cultured under hypoxia (1% O₂). After 72 h from the addition of test compounds, cell growth was evaluated by using the WST-8 cell counting kit (Dojindo) according to manufacturer's instructions. Absorbance was measured at 450 nm in a microplate reader (Bio-rad).

4.2.3. RNA extraction and quantitative real-time PCR

Total RNA of HT1080 cells was isolated using Total RNA Extraction kit (Viogene). cDNA was reverse transcribed from 0.5 μ g of the total RNA using ReverTra Ace α (TOYOBO) using a random primer. For the quantitative real-time PCR, DNA amplification was carried out using the Fast Start Universal SYBR Green Master (ROX) (Roche). Primers used for PCR were as follows: human CA-IX, 5'-ACCCTC TCTGACACCCTGTG-3' (sense) and 5'-GGCTGGCTTCTCACATTCTC-3' (antisense); human HIF-1 α , 5'-TACTAGCTTTGCAGAATGCTC-3' (sense) and 5'-GCCTTGATAGGAGCATTAAAC-3' (antisense); human HIF-1 β , 5'-GGGGCAGCTTACCTCTAAC-3' (sense) and 5'-GGGTA GAGCACTCGAACTG-3' (antisense); human 18S rRNA, 5'-GCAATTATCCCATGAACG-3'(sense) and 5'-GGGACTTAATCAA CGCAAGC-3' (antisense).

Relative expression level was calculated by the $\Delta\Delta$ CT method, and normalized with 18S rRNA level.

4.2.4. Wound-healing assay

HT1080 cells were plated at 7.5×10^4 cells per well in a 6-well plate. When the cells were confluent, a monolayer of the cells was scratched using a sterile 200 μ l pipette tip. After replacing the medium with fresh medium to remove cell debris, vehicle or the test compound was added to the cells, followed by an additional

24 h incubation under hypoxia. Images of scratch-wound were acquired using phase contrast microscopy.

Acknowledgements

We thank Drs. H. Osada (RIKEN) and M. Hiraoka (Kyoto University) for providing x5HRE/HT1080 cells and a 5xHRE/pGL3/VEGF/E1b reporter plasmid, respectively. We are also grateful to Mrs. M. Morioka and E. Moriyoshi (Kyoto University) for supporting the HIF-1 inhibitor screening. This work was supported in part by research grants from the Japan Society for the Promotion of Science (JSPS), the Ministry of Education, Culture, Sports, Science and Technology of Japan (MEXT), the Ministry of Health, Labour and Welfare of Japan (MHLW).

Supplementary data

Supplementary data associated with this article can be found, in the online version, at <http://dx.doi.org/10.1016/j.bmc.2015.02.038>.

References and notes

1. Semenza, G. L. *Oncogene* **2010**, *29*, 625.
2. Semenza, G. L. *Nat. Rev. Cancer* **2003**, *3*, 721.
3. Xia, Y.; Choi, H. K.; Lee, K. *Eur. J. Med. Chem.* **2012**, *49*, 24.
4. Ban, H. S.; Uto, Y.; Nakamura, H. *Expert Opin. Ther. Pat.* **2011**, *21*, 131.
5. Li, S. H.; Shin, D. H.; Chun, Y. S.; Lee, M. K.; Kim, M. S.; Park, J. W. *Mol. Cancer Ther.* **2008**, *7*, 3729.
6. Harada, H.; Inoue, M.; Itasaka, S.; Hirota, K.; Morinibu, A.; Shinomiya, K.; Zeng, L.; Ou, G.; Zhu, Y.; Yoshimura, M.; McKenna, W. G.; Muschel, R. J.; Hiraoka, M. *Nat. Commun.* **2012**, *3*, 783.
7. Mallena, S.; Lee, M. P. H.; Bailly, C.; Neidle, S.; Kumar, A.; Boykin, D. W.; Wilson, W. D. *J. Am. Chem. Soc.* **2004**, *126*, 13659.
8. Wai, J. S.; Egbertson, M. S.; Payne, L. S.; Fisher, T. E.; Embrey, M. W.; Tran, L. O.; Melamed, J. Y.; Langford, H. M.; Guare, J. P., Jr.; Zhuang, L.; Grey, V. E.; Vacca, J. P.; Holloway, M. K.; Naylor-Olsen, A. M.; Hazuda, D. J.; Felock, P. J.; Wolfe, A. L.; Stillmock, K. A.; Schleif, W. A.; Gabryelski, L. J.; Young, S. D. *J. Med. Chem.* **2000**, *43*, 4923.
9. Waring, M. J. *Expert Opin. Drug Discovery* **2010**, *5*, 235.
10. Shin, D. H.; Kim, J. H.; Jung, Y. J.; Kim, K. E.; Jeong, J. M.; Chun, Y. S.; Park, J. W. *Cancer Lett.* **2007**, *255*, 107.
11. Teague, S. J.; Davis, A. M.; Leeson, P. D.; Oprea, T. *Angew. Chem., Int. Ed.* **1999**, *38*, 3743.
12. Shibata, T.; Akiyama, N.; Noda, M.; Sasai, K.; Hiraoka, M. *Int. J. Radiat. Oncol. Biol. Phys.* **1998**, *42*, 913.

Tolerability of Nintedanib (BIBF 1120) in Combination with Docetaxel: A Phase 1 Study in Japanese Patients with Previously Treated Non–Small-Cell Lung Cancer

Isamu Okamoto, MD, PhD,*† Masaki Miyazaki, MD, PhD,*‡ Masayuki Takeda, MD, PhD,* Masaaki Terashima, MD, PhD,*§ Koichi Azuma, MD, PhD,*|| Hidetoshi Hayashi, MD, PhD,*¶ Hiroyasu Kaneda, MD, PhD,* Takayasu Kurata, MD, PhD,*# Junji Tsurutani, MD, PhD,* Takashi Seto, MD, PhD,** Fumihiko Hirai, MD, PhD,** Koichi Konishi, BPharm,†† Akiko Sarashina, MSc,‡‡ Nobutaka Yagi, MSc,†† Rolf Kaiser, MD,§§ and Kazuhiko Nakagawa, MD, PhD*

Background: This phase I, open-label study evaluated the safety/tolerability and maximum tolerated dose of second-line nintedanib combined with docetaxel in Japanese patients with advanced non-small-cell lung cancer.

Methods: Eligible patients received docetaxel 60 or 75 mg/m² (day 1) plus nintedanib 100, 150, or 200 mg twice daily (bid; days 2–21) in 21-day cycles. Standard 3 + 3 dose escalations were performed separately in patient cohorts with a body surface area (BSA) of less than 1.5 m² (BSA <1.5) and BSA greater than or equal to 1.5, respectively.

Results: Forty-two patients (17 BSA <1.5, 25 BSA ≥1.5) were treated. The maximum tolerated dose of nintedanib was 150 and 200 mg bid in patients with BSA less than 1.5 and BSA greater than or equal to 1.5 (BSA ≥1.5), respectively, in combination with 75 mg/m² of docetaxel. Dose-limiting toxicities (all grade 3 hepatic enzyme elevations) occurred in 12 patients (six per cohort). Drug-related adverse

events included neutropenia (95%), leukopenia (83%), fatigue (76%), alopecia (71%), decreased appetite (67%), and elevations in alanine aminotransferase (64%) and aspartate aminotransferase (64%). All hepatic enzyme elevations were reversible and manageable with dose reduction or discontinuation. Among 38 evaluable patients, 10 (26%) had a partial response and 18 (47%) had stable disease.

Conclusion: Continuous treatment with second-line nintedanib combined with docetaxel was manageable and showed promising signs of efficacy in Japanese patients with advanced non-small-cell lung cancer.

Key Words: Clinical trials, Phase I, Docetaxel, Japanese, Nintedanib, Non-small-cell lung cancer, Pharmacokinetics.

(*J Thorac Oncol.* 2015;10: 346–352)

Few treatment options are available for patients with advanced non-small-cell lung cancer (NSCLC) who fail first-line chemotherapy. Currently, the only licensed second-line therapies for individuals with NSCLC, who do not harbor identifiable driver oncogenes, such as sensitizing epidermal growth factor receptor (*EGFR*) gene mutations or anaplastic lymphoma kinase (*ALK*) gene translocations, are docetaxel, gemcitabine, pemetrexed (for nonsquamous NSCLC), and erlotinib.¹ Although these treatments are efficacious, survival benefits are modest. Hence, there is an urgent need for effective and well-tolerated second-line options.

Angiogenesis plays an important role in the development and differentiation of NSCLC.² Targeting vascular endothelial growth factor (VEGF) signaling appears to be particularly important in advanced NSCLC, given the proven efficacy of the VEGF-targeted monoclonal antibody bevacizumab as first-line therapy in large-scale trials.^{3,4} However, to date no oral tyrosine kinase inhibitors of VEGF receptors have been approved for the treatment of advanced NSCLC. Mechanisms that support solid tumor angiogenesis include VEGF, fibroblast growth factor, and platelet-derived growth factor signaling pathways.^{5–8} Nintedanib (BIBF 1120) is a potent, oral, small-molecule triple angiokinase inhibitor that targets VEGF receptors 1 to 3, platelet-derived growth factor

*Department of Medical Oncology, Kinki University Faculty of Medicine, Osaka, Japan; †Center for Clinical and Translational Research, Faculty of Medicine, Kyusyu University Hospital, Fukuoka, Japan; ‡Department of Internal Medicine, Suita Municipal Hospital, Osaka, Japan; §Department of Medical Oncology, Nara Hospital, Kinki University Faculty of Medicine, Nara, Japan; ||Department of Medicine, Division of Respiriology, Neurology, and Rheumatology, Kurume University Hospital, Fukuoka, Japan; ¶Department of Medical Oncology, Kishiwada Municipal Hospital, Osaka, Japan; #Department of Thoracic Oncology, Kansai Medical University, Hirakata Hospital, Osaka, Japan; **Department of Medical Oncology, National Kyushu Cancer Centre, Fukuoka, Japan; ††Department of Medical Oncology, National Kyushu Cancer Centre, Fukuoka, Japan; ‡‡Nippon Boehringer Ingelheim Co. Ltd., Medical Development Division, Hyogo, Japan; and §§Clinical Pharmacokinetics/Pharmacodynamics Department, Boehringer Ingelheim Pharma GmbH & Co. KG, Biberach, Germany.

Funding: This work was supported by Boehringer Ingelheim.

K.K., A.S., and N.Y. are employees of Nippon Boehringer Ingelheim Co. Ltd.; R.K. is an employee of Boehringer Ingelheim Pharma GmbH & Co.; T.S. has received honoraria from Boehringer Ingelheim and is a member of their speaker bureau; all remaining authors have declared no conflict of interest.

Address for correspondence: Isamu Okamoto, MD, PhD, Center for Clinical and Translational Research, Kyushu University Hospital, 3-1-1 Maidashi, Higashiku, Fukuoka 812-8582, Japan. E-mail: okamotoi@kokyu.med.kyushu-u.ac.jp

DOI: 10.1097/JTO.0000000000000395

Copyright © 2014 by the International Association for the Study of Lung Cancer
ISSN: 1556-0864/15/1002-0346

receptors alpha and beta, and fibroblast growth factor receptors 1 to 3, besides RET and Flt3.⁹ Preclinical experiments have shown that nintedanib can delay tumor growth and inhibit angiogenesis in various xenograft models of human cancer, including NSCLC.⁹ More recently, the global LUME-Lung 1 phase III trial (Study 1199.13; NCT00805194) for previously treated advanced NSCLC demonstrated that treatment with a combination of nintedanib and docetaxel produced a significant and clinically meaningful improvement in overall survival compared with docetaxel and placebo in predefined patients with adenocarcinoma tumor histology.¹⁰

In a recent Japanese phase I study, the maximum tolerated dose (MTD) of nintedanib monotherapy was 200 mg bid, which is lower than the MTD of 250 mg bid for Caucasian patients.^{11,12} Although the reason for this difference remains unclear, analogous differences in the tolerability of chemotherapy for advanced NSCLC between Japanese and US patients have been reported previously, and have been related to differences in genotypic variants between the two populations.¹³ In addition, the standard dose of docetaxel 60 mg/m² commonly employed for Japanese patients with advanced NSCLC¹⁴ is lower than the 75 mg/m² dose used for Western populations.^{10,15} This phase I dose-escalation study (Study 1199.29; NCT00876460) was conducted to define the MTD of nintedanib combined with docetaxel, and to confirm the safety/tolerability profile of the combination in Japanese patients with advanced NSCLC following failure of first-line platinum-based chemotherapy.

PATIENTS AND METHODS

Study Population

Patients aged 20 to 74 years with histologically or cytologically confirmed, advanced stages IIIB to IV or recurrent NSCLC (any histology) who had received one platinum-based chemotherapy regimen (not containing docetaxel) were enrolled. Patients had an Eastern Cooperative Oncology Group performance status of 0 to 1, a life expectancy exceeding 3 months, and adequate organ function. Exclusion criteria included: active brain metastases; gastrointestinal disorders that could interfere with the absorption of the study drug; history of major thrombotic or clinically relevant major bleeding event in the past 6 months; clinically significant hemoptysis in the past 3 months; active multiple primary neoplasms; or significant cardiovascular disease.

Study Design

This open-label trial utilized a standard 3 + 3 dose-escalation design. Eligible patients received intravenous docetaxel at a dose of 60 mg/m² or 75 mg/m² on day 1, followed by continuous, oral nintedanib bid on days 2 to 21 in 21-day cycles. Nintedanib was started at a dose of 100 mg bid and escalated up to 200 mg bid in 50 mg bid intervals. Continuous nintedanib monotherapy was permitted in cases where docetaxel had to be permanently discontinued for reasons other than progression, and the patient had already received at least four treatment cycles of combination therapy.

Dose-limiting toxicity (DLT) was defined as nonhematologic toxicity greater than Common Terminology Criteria for

Adverse Events (CTCAE) grade 3, excluding electrolyte abnormalities or isolated elevations of γ -glutamyl transpeptidase (γ -GT); grade 3 or higher gastrointestinal toxicity or hypertension despite optimal supportive care/intervention; grade 4 neutropenia for more than 7 days despite optimal supportive care; grade 4 febrile neutropenia of any duration; grade 2 or higher alanine aminotransferase (ALT) and/or aspartate aminotransferase (AST) elevations combined with grade 2 or higher bilirubin elevations; inability to resume nintedanib dosing within 14 days of stopping treatment due to treatment-related toxicity. DLTs observed in the first 21 days of treatment were used to determine MTD, defined as the highest dose at which incidence of DLTs in cycle 1 was less than or equal to 33.3%.

After testing nintedanib 100 mg bid plus docetaxel 60 mg/m² (N100/D60), nintedanib 150 mg bid plus docetaxel 60 mg/m² (N150/D60), and nintedanib 200 mg bid plus docetaxel 60 mg/m² (N200/D60) without considering body surface area (BSA), dose escalations were performed separately in two patient cohorts with a BSA of less than 1.5 m² (BSA <1.5) and greater than or equal to 1.5 m² (BSA \geq 1.5), respectively. This protocol amendment was recommended by the external Efficacy and Safety Review Committee following early observation of a high incidence of DLTs in patients with a BSA of less than 1.5 m².

The institutional review board reviewed and approved the protocol and its amendments. The trial was conducted in compliance with the study protocol, the Declaration of Helsinki, and Good Clinical Practice guidelines. All patients provided written informed consent.

Assessments

Adverse events (AEs) were assessed according to CTCAE version 3.0 throughout the trial and for 28 days after treatment cessation. All safety analyses were undertaken in patients who had received 1 dose or more of nintedanib. Objective tumor response was evaluated according to the Response Evaluation Criteria in Solid Tumors (RECIST 1.0). Tumor assessment was performed at screening and every 6 weeks on day 1 (within 7 days) of each odd-numbered treatment cycle (cycles 3, 5, etc.). Hematology and biochemistry assessments were undertaken at screening and at predefined intervals during the trial.

To investigate the possible effect of nintedanib on the pharmacokinetics (PK) of docetaxel, blood samples were taken predose and 1, 1.5, 2, 3, 4, 7, 24, and 48 hours post-dose on days 1 to 3 of cycles 1 and 2. Sampling for PK characterization of nintedanib was carried out on days 2 to 3 of cycle 1, with samples taken predose, 1, 2, 3, 4, 6, 7, 10, and 24 hours after the morning dose. Samples for evaluation of trough concentrations of nintedanib were taken on days 8 and 15 of the first two cycles, and on days 1 to 3 during cycle 2, before the morning dose. All PK analyses were carried out using WinNonlin software, applying a noncompartmental approach.

Statistical Analysis

The primary end points were the determination of the MTD of nintedanib in combination with docetaxel at doses

of 60 or 75 mg/m², and the assessment of the frequency and severity of AEs. Secondary end points included PKs of nintedanib and docetaxel, best tumor response and progression-free survival (PFS). Descriptive statistics are presented.

RESULTS

Patients

A total of 43 patients with advanced NSCLC were enrolled into this study from March 2009 to August 2012. One patient discontinued due to a non-DLT adverse event before the first dose of nintedanib was administered and was excluded from the study. Baseline characteristics, except for gender and clinical stage, were similar between the two BSA cohorts (Table 1).

At the time of the database lock (June 11, 2013), all 42 patients had discontinued combination treatment. Reasons for discontinuation included progressive disease (*n* = 22), AEs (*n* = 14), and withdrawal of consent (*n* = 3). Three patients continued to be treated with nintedanib monotherapy after discontinuation of docetaxel due to drug-related AEs (grade 1 and 2 peripheral neuropathy in two patients, and grade 2 pleural effusion in one patient). Median (range) number of days of treatment administered was 126.5 (7–1339).

Maximum Tolerated Dose and Dose-Limiting Toxicities

The allocation of patients to treatment during the study is summarized in Figure 1. Of the 42 patients who received nintedanib treatment, three patients were excluded from the DLT assessment due to low compliance with study treatment: one excluded patient had a non-DLT adverse event,

TABLE 1. Patient Characteristics at Baseline and Treatment Allocation

	Patients with BSA <1.5 m ² (<i>n</i> = 17)	Patients with BSA ≥1.5 m ² (<i>n</i> = 25)	All Patients (<i>n</i> = 42)
Age, years			
Median (range)	65 (45–72)	62 (47–73)	64 (45–73)
Gender, <i>n</i> (%)			
Male	6 (35)	23 (92)	29 (69)
Female	11 (65)	2 (8)	13 (31)
ECOG performance score, <i>n</i> (%)			
0	6 (35)	8 (32)	14 (33)
1	11 (65)	17 (68)	28 (67)
Clinical stage, <i>n</i> (%)			
IIIB	1 (6)	6 (24)	7 (17)
IV	16 (94)	19 (76)	35 (83)
Histology, <i>n</i> (%)			
Adenocarcinoma	14 (82)	19 (76)	33 (79)
Squamous cell carcinoma	3 (18)	5 (20)	8 (19)
Large-cell carcinoma	0	1 (4)	1 (2)

bid, twice daily; BSA, body surface area; D, docetaxel; DLT, dose-limiting toxicity; ECOG, Eastern Cooperative Oncology Group; N, nintedanib.

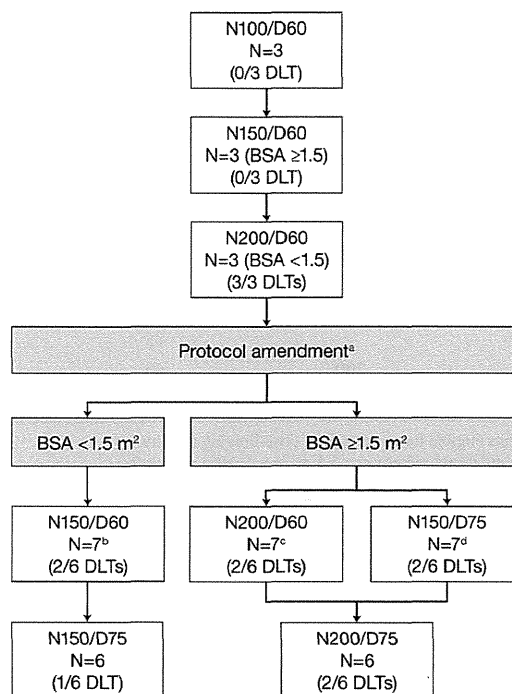


FIGURE 1. Patient flow. N100/D60, nintedanib 100 mg bid plus docetaxel 60 mg/m²; N150/D60, nintedanib 150 mg bid plus docetaxel 60 mg/m²; N150/D75, nintedanib 150 mg bid plus docetaxel 75 mg/m²; N200/D60, nintedanib 200 mg bid plus docetaxel 60 mg/m²; N200/D75, nintedanib 200 mg bid plus docetaxel 75 mg/m². ^aProtocol amendment by the Efficacy and Safety Review Committee, which recommended separate assessments of dose levels for patients with a body surface area (BSA) <1.5 m² and ≥1.5 m². ^bOne patient was replaced due to low compliance with study drugs administration with a non-dose-limiting toxicity adverse event (pneumonia). ^cOne patient was replaced due to insufficient data to evaluate the duration of grade 4 neutropenia as a dose-limiting toxicity. ^dOne patient was replaced due to early withdrawal of consent.

the second patient withdrew consent before the completion of cycle 1, and there were insufficient data to confirm a DLT occurrence in the third patient. Three patients were enrolled in the N100/D60 cohort, three patients in the N150/D60 cohort, and three patients in the N200/D60 cohort, without consideration of their BSA. No DLT was observed for the first and second cohorts (N100/D60 and N150/D60). At 200 mg bid (N200/D60), all three patients experienced DLTs (ALT, AST, and γ -glutamyltransferase increases in two patients, and ALT and AST increase in one patient) that were fully reversible (Table 2). All three patients who experienced DLTs at N200/D60 had BSA less than 1.5, whereas the three patients treated with N150/D60 who did not experience DLTs had BSA greater than or equal to 1.5. In a previous investigation of nintedanib monotherapy in Japanese patients,¹¹ all DLTs at 200 mg bid were observed in patients whose BSAs were smaller than those of patients without observed DLTs. The external Efficacy and Safety Review Committee recommended the protocol amendments for reassessment of